Theoretical Study of the Internal Charge Transfer in Aminobenzonitriles

Luis Serrano-Andrés,[†] Manuela Merchán,[†] Björn O. Roos,*[,‡] and Roland Lindh[‡]

Contribution from the Departamento de Química Física, Universidad de Valencia, Dr. Moliner 50, Burjassot, E-46100 Valencia, Spain, and Department of Theoretical Chemistry, Chemical Centre, P.O.B. 124, S-221 00 Lund, Sweden

Received February 10, 1994. Revised Manuscript Received May 2, 1994[⊗]

Abstract: The lower excited states for the molecules aminobenzonitrile (ABN) and (dimethylamino)benzonitrile (DMABN) have been studied as a function of the twisting and wagging motion of the amino group. Theoretical calculations have been performed using the complete active space (CAS) SCF method in combination with multiconfigurational second order perturbation theory (CASPT2). Basis sets of the ANO-type (C,N/3s2p1d and H/2s) were employed. Ground state geometries were optimized at the CASSCF level. The excitation energies were computed as function of a twist angle, where the amino group is rotated with respect to the benzonitrile plane, and for two values of the wagging angle (0 and 21°). The influence of the wagging angle in the nontwisted molecules was also analyzed. The results fully confirm the twist intramolecular charge transfer (TICT) model proposed to explain the dual fluorescence phenomena occurring in DMABN. The absence of the low frequency part of the fluorescence spectrum in ABN in explained by the shape of the potential energy surface along the isomerization path, due to the large energy gaps among the interacting states, which prevents the amino group from rotating into the TICT state. Calculated transition energies (absorption and emission), structural, and electrical properties of the ground and excited states are in agreement with available experimental information.

1. Introduction

Dual fluorescence occurring in different exciplex, excimer, and proton-transfer systems is by now a now well-documented phenomenon since the discovery by Lippert *et al.*[1] of the dual fluorescence in (*p*-dimethylamino)benzonitrile (DMABN) (*p*-cyano-*N,N*-dimethylamine) in dilute solutions and polar solvents. The second fluorescence band has since then been found in numerous electron donor−acceptor molecules where the two moieties are linked by a single bond,[2] even in organometallic and inorganic compounds. Many spectroscopic, thermodynamic, and quantum-chemical studies have been devoted to these systems, and their prospective role in photochemistry and photobiology has been analyzed. The large charge separation, which is present in the excited states, has also been widely studied. Mulliken[3] introduced the concept of charge transfer transition, *i.e.*, the transfer of an electron from a donor to an acceptor by means of a direct excitation or by electron transfer between two moieties when either of them are excited. The high reactivity of these radical or strongly polar states makes them play an important role in the understanding of the primary mechanisms of vision and photosynthesis.[2−5]

Different models have been proposed to account for the dual fluorescence. Lippert *et al.*[1] primarily suggested emission from two low-lying singlet states and their inversion by interaction with the solvent; McGlynn *et al.*[6] proposed the formation of an excimer; Kosower *et al.*[7] considered the possibility of a proton transfer in the excited state, while Chandross[8] and Visser *et al.*[9] suggested, respectively, complexation or formation of exciplexes with the solvent. Although the exciplex hypothesis is still defended,[10] strong arguments have been raised against a main role of solute−solvent complexes in explaining the dual fluorescence of aminobenzonitriles.[11−13] Recently, a new model based on solvent-induced vibronic coupling between the low-lying singlet states has been proposed.[14,15] The most accepted model used to explain the dual fluorescence supports, however, a "twisted intramolecular charge transfer" state as being responsible for the lower-energy fluorescence band. The model was proposed and coined with the acronym TICT by Gabrowski *et al.*[16,17] 20 years ago.

[†] Universidad de Valencia.

[‡] Chemical Centre.

[⊗] Abstract published in *Advance ACS Abstracts,* March 1, 1995.

(1) Lippert, E.; Lüder, W.; Moll, F.; Nägele, W.; Boos, H.; Prigge, H.; Seibold-Blankenstein, I. *Angew. Chem.* **1961**, *73*, 695. Lippert, E.; Lüder, W.; Boos, H. In *Advances in Molecular Spectroscopy*; Mangini, A., Ed.; Pergamon Press: Oxford, 1962; p 443.

(2) Rettig, W. *Angew. Chem.* **1986**, *98*, 969; *Angew. Chem., Int. Ed. Engl.* **1986**, *25*, 971.

(3) Mulliken, R. S. *J. Am. Chem. Soc.* **1950**, *72*, 600; **1952**, *74*, 811; *J. Phys. Chem.* **1952**, *56*, 801.

(4) Cowley, D. J. *Nature* **1986**, *319*, 14.

(5) Bonacić-Koutecký, V.; Koutecký, J.; Michl, J. *Angew. Chem., Int. Ed. Engl.* **1987**, *26*, 170.

(6) Khalil, O. S.; Hofeldt, R. H.; McGlynn, S. P. *Chem. Phys. Lett.* **1972**, *17*, 479.

(7) Dodiuk, H.; Kosower, E. M. *Chem. Phys. Lett.* **1975**, *34*, 253. Kosower, E. M.; Dodiuk, H. *J. Am. Chem. Soc.* **1976**, *98*, 924.

(8) Chandross, E. A. In *Exciplex*; Gordon, M.; Ware, W. R.; Eds.; Academic Press: New York, 1975; p 187.

(9) Visser, R. J.; Varma, C. A. *J. Chem. Soc., Faraday Trans. II* **1980**, *76*, 453. Visser, R. J.; Weisenbom, P. C. M.; Varma, C. A. *Chem. Phys. Lett.* **1985**, *113*, 330. Weisenborn, P. C. M.; Varma, C. A.; de Haas, M. P.; Warman, J. M. *Chem. Phys. Lett.* **1986**, *129*, 560.

(10) Delange, M. C. C.; Leeson, D. T.; Vankuijk, K. A. B.; Huizer, A. H.; Varma, C. A. *Chem, Phys.* **1993**, *174*, 425.

(11) Kobayashi, T.; Futakami, M.; Kajimoto, O. *Chem. Phys, Lett.* **1986**, *130*, 63. Kajimoto, O.; Futakami, M.; Kobayashi, T.; Yamasaki, K. *J. Chem. Phys.* **1988**, *92*, 1347.

(12) Rulliére, C.; Grabowski, Z. R.; Dobkowski, J. *Chem. Phys. Lett.* **1987**, *137*, 408.

(13) Leinhos, U.; Kühnle, W.; Zachariasse, K. A. *J. Phys. Chem.* **1991**, *95*, 2013.

(14) Zachariasse, K. A.; von der Haar, T.; Hebecker, A.; Leinhos, U.; Kühnle, W. *Pure Appl. Chem.* **1993**, *65*, 1745.

(15) Zachariasse, K. A.; von der Haar, Th.; Hebecker, A.; Leinhos, U.; Kühnle, W. *XIIth International Conference on Photochemistry*; Vancouver, Canada, Aug 1−6, 1993.

(16) Rotkiewicz, K.; Grellmann, K. H.; Grabowski, Z. R. *Chem. Phys. Lett.* **1973**, *19*, 315; **1973**, *21*, 212.

0002-7863/95/1517-3189$09.00/0

The TICT model[16-18] explains the dual fluorescence as occurring by means of an adiabatic photoreaction or horizontal radiationless transition leading to two conformations of the same molecule differing in the dihedral angle comprising the amino group and the phenyl ring. The initially promoted state would yield another minimum on the energy surface by twisting the dialkylamine group from a nearly planar to a perpendicular position with respect to the benzonitrile plane. The twisting would be connected with the transfer of one unit of charge from the amine to the aromatic or cyano group, and the excited state at the twisted position would formally be a charge transfer (CT) state with a large intramolecular charge separation and an increased dipole moment. The state would stabilize in polar solvents. From the start, the "anomalous" lower-energy band, also named F_A or A band, was assigned to fluorescence from the more polar CT, A* or ^1L_a-type state (Platt's nomenclature[19]), while the "expected" emission band, F_B or B band, was assigned to the less polar LE (locally excited), B* or ^1L_b-type state.[1] The evidence for the assignments were, however, not conclusive. The fluorescence and absorption polarization measurements by Lippert *et al.*,[1] confirmed by later experiments in several solvents,[18,20-22] showed that the main absorption and higher-energy fluorescence (F_B) bands are long-axis polarized (A symmetry within the C_2 framework), although the edges of the bands are polarized in a direction perpendicular to the long axis (B symmetry). This point illustrates that both the absorption and the F_B band have a mixed polarization. Therefore, while the most intense absorption comes to a state of A symmetry, the initial state for the photoreaction has B symmetry. The A state should be considered the initially promoted state, not as the lowest-energy state in the absorption (which has B symmetry as shown by the polarization experiments), but as the state which carries most of the energy in the absorption by its allowed Franck–Condon character. Polarization measurements and oscillator strength values confirm this point. The F_B fluorescence band starts with a B-type polarization to reach an A-type polarization at the maximum of the band due to the vibronic mixing and to the thermal activation of the fluorescence, as was shown by the single point measurement made by Grabowski *et al.*[16] in glycerol. The low-energy fluorescence (F_A) band, however, is strongly polarized along the long axis of the molecule and thus arises by emission from an excited state of A symmetry.

The TICT model is supported by a large amount of experimental data. Compounds with a fixed molecular framework where the amino group rotation toward the TICT geometry is inhibited by molecular bridging do not yield a second fluorescence band.[23-25] Moreover, other systems with the planar conformation made unavailable by steric hindrance, only give the lower energy emission.[26-29] Recent studies on these and related molecules[13,14] have shown that the mechanism is not completely understood, due to the presence of ICT on molecules without flexibility to reach a 90° twisting and the different efects of the solvent in other systems. It is clear that the order of the excited states and their behavior on the isomerization motions should be carefully analyzed. Most of the investigations have been carried out in liquid solutions. The importance of the solvent in the emission mechanism has been especially considered due to the extreme sensibility of the lower-energy band wavelength and intensity on the solvent polarity. Dual fluorescence has been detected in nonpolar solvents,[30] and electro-optical emission measurements for several molecules in gas-phase[2,28,29] have been capable of detecting the ICT state by analyzing the emission under the influence of an electrical field. Thus, the existence of a solvent-free mechanism has been established in some systems, although not in DMABN, where the presence of highly polar (diethyl ether or more polar) or polarizable solvents (toluene) seems necessary to yield the dual fluorescence. The large dipole moments measured for the ICT state[30] and the observation of a benzonitrile anion-like species in picosecond transient absorption spectroscopy of the polar state of DMABN and some derivatives[12,31] also strongly support the reorientation relaxation model.

The most severe criticism against the TICT mechanism comes from the fact that the initial evidence for a strong dependence of the fluorescence with the viscosity of the solvent[26] turned out to be an experimental artifact.[32] A viscosity dependence in the relative rotational dynamics of the dialkylamino group is expected but has not been shown by the reaction rates.[32,33] Experimental evidence[32-34] indicates that the ICT reaction in DMABN and related molecules is mainly influenced by solvent polarity and not so much by solvent viscosity. This also seems to be the case for (dialkylamino)benzonitriles with longer alkyl groups.[21] However, the degree of twisting that accompanies the charge transfer reactions has not been definitely established. Therefore, another evidence used to question the relationship between the twisting angle and the ICT mechanism[35] is that the S_1 state seems to have an energy minimum at a twist angle of about 30°. This argument hardly invalidates the TICT model if the twist starts in the S_2 state at the nontwisted geometry. Even more, if the S_1 state had a local minimum around 30° of twisting, this oculd be related with the LE emission band, and only a small amount of twisting would be required to cross over from the LE to the TICT surface, once the expected activation barrier between the minima is overcome. In addition, if an efficient charge separation is already present at small twisting angles on the S_1 surface, the relaxation to the equilibrium twisted geometry can be developed after a partial charge transfer. In this case, little or no viscosity dependence would be expected. It has been previously reported that the TICT emission spectra of some dialkylaminophenylsulfones exhibit a time-dependent Stokes shift. The spectral evolution has been interpreted in terms of the time-dependent relaxation of the solvent following the electron transfer.[33] The study of

(17) Siemiarczuk, A.; Grabowski, Z. R.; Krowczyński, A.; Asher, M.; Ottolengui, M. *Chem. Phys. Lett.* **1977**, *51*, 315.
(18) Lippert, E.; Rettig, W.; Bonačić-Kouteký, V.; Heisel, F.; Miehé, J. A. *Adv. Chem. Phys.* **1987**, *68*, 1.
(19) Platt, J. R *J. Chem. Phys.* **1949**, *17*, 484.
(20) Lippert, E.; Rettig, W. *J. Mol. Struct.* **1978**, *45*, 373.
(21) Zachariasse, K. A. private communication.
(22) Grabowski, Z. R., private communication.
(23) Rotkiewicz, K.; Grabowski, Z. R.; Krowczyński, A.; Kühnle, W. *J. Lumin.* **1976**, *12–13*, 877.
(24) Rettig, W.; Rotkiewicz, K.; Rubaszewska, W. *Spectrochim. Acta* **1984**, *40A*, 241.
(25) Wermuth, G.; Rettig, W. *J. Phys. Chem.* **1984**, *88*, 2729. Rettig, W.; Gleiter, R. *J. Phys. Chem.* **1985**, *89*, 4676.
(26) Grabowski, Z. R.; Rotkiewicz, K.; Siemiarczuk, A.; Cowley, D. J.; Baumann, W. *Nouv. J. Chim.* **1979**, *3*, 443.
(27) Rettig, W.; Marschner, F. *Nouv. J. Chim.* **1983**, *7*, 425.
(28) Bischof, H.; Baumann, W.; Detzer, N.; Rotkiewicz, K. *Chem. Phys. Lett.* **1985**, *116*, 180.
(29) Rotkiewicz, K.; Rubaszawska, W. *Chem. Phys. Lett.* **1980**, *70*, 444; *J. Lumin.* **1982**, *27*, 221.
(30) Schuddeboom, W.; Jonker, S. A.; Varman, J. M.; Leinhos, V.; Kühnle, W.; Zachariasse, K. A. *J. Phys. Chem.* **1992**, *96*, 10809.
(31) Okada, T.; Mataga, N.; Baumann, W.; Siemiarczuk, A. *J. Phys. Chem.* **1987**, *91*, 4490. Okada, T.; Mataga, N.; Baumann, W. *J. Phys. Chem.* **1987**, *91*, 760.
(32) Hicks, J.; Vandersall, M.; Babagoric, Z.; Eisenthal, K. B.; *Chem. Phys. Lett.* **1985**, *116*, 18. Hicks, J.; Vandersall, M.; Sitzmann, E. V.; Eisenthal, K. B. *Chem. Phys. Lett.* **1987**, *135*, 413.
(33) Simon, J. D.; Su, S. G. *J. Phys. Chem.* **1990**, *94*, 3656.
(34) Kajimoto, O.; Nayuki, T.; Kobayashi, T. *Chem. Phys. Lett.* **1993**, *209*, 357.
(35) Grassian, V. H.; Warren, J. A.; Bernstein, E. R.; Secor. H. V. *J. Chem. Phys.* **1989**, *90*, 3994.

the ICT reaction of DMABN[30] showed, however, that the charge transfer reaction in toluene is slower than the solvent relaxation, maybe because of the large rotation, and also that the ICT state cannot be reached directly by absorption from the ground state, which has been shown to occur for DMABN in supercritical fluids.[34] The experimental evidence indicates, therefore, absence of the pure CT state at the moment of the excitation. A crossing of the S_2 (2^1A) state with the higher charge transfer state will take place along a relaxation path in order to yield the lower emission from the CT state. In other systems, like cyanobenzoquinuclidine, the CT state seems to be the lowest in polar solvents and can be directly reached from the ground state.[21]

An alternative explanation of the dual fluorescence has recently been put forward,[14] which is based on solvent-induced vibronic coupling between the LE and the CT states. A condition for this coupling is a small energy gap between the two states. Zachariasse *et al.*[13-15,21,30] propose the N-inversion of the amino group acting as the promoting mode, which decouples, even without rotational isomerization, the nitrogen lone-pair from the π electrons of the phenyl ring. This is suggested to lead to an increase in the localization of the positive charge on the amino group and, hence, to a larger value of the dipole moment of the CT state. The present theoretical study does not lend support to such an alternative mechanism, although some of its statements cannot be completely ruled out. Most of the effects observed in different systems where new substituents have been added on the amino group or the benzonitrile moiety are without doubt more related to the energy gap between the LE (B) and CT (A) states and the shapes of the potential energy surfaces than, for instance, the suggested pretwist angles in the ground state. The wagging motion of the alkylamino group is also important in order to arrive at a more complete understanding of the mechanism. However, as will be shown in the paper, the wagging motion without twisting cannot explain the large charge transfer and dipole moments, which have been measured. The original TICT process is the only one, which agrees with these observations. It is obvious that a quantum-chemical calculation related to isolated molecules in gas-phase cannot speak conclusively against a dynamic process such as the proposed solvent-induced pseudo-Jahn-Teller mechanism.[13-15,21,30] Nevertheless, the present theoretical findings show that a wagging motion based on the N inversion is clearly unable to produce the charge transfer expected for the lower-energy fluorescence in DMABN, while the twisting motion leads to a transfer of charge in agreement with experimental evidence. No other model has been proposed which accounts better for the observations. A detailed knowledge of the structure of at least three potential surfaces is necessary for the understanding of the ICT process in a given system. Small differences in the structure easily lead to a different behavior. It is therefore clear that a detailed knowledge of the surface shapes, energies, and the nature of the electronic wave functions is needed in order to fully understand the phenomenon of dual fluorescence in a given system. The present work demonstrates that TICT is a very plausible mechanism for the explanation of the process in the molecules ABN and DMABN. It is not unlikely that other mechanisms may be active in systems not directly related to these.

Theoretical studies on the key systems are available using both semiempirical and *ab initio* methods. Most of the semiempirical studies have confirmed the validity of the general features of the TICT model,[36-41] although there are counter examples.[42] *Ab initio* calculations[37,43] have been performed at too low a level of theory to obtain conclusive quantitative results. The effect of the solvent has been considered theoretically with diverging results.[41,43-45] *Ab initio* studies at a higher level have only been possible for smaller analogue molecules such as aminoborane H_2N-BH_2, where MRCI calculations[46] gave evidence for a charge-separated S_1 state at a perpendicular geometry. Other donor-acceptor systems with zwitterionic excited states have been studied, and their structure has been explained within the same model.[5,18] Calculations at an adequate level of theory are necessary in order to explain the dual fluorescence process also in larger molecules and to clarify how the charge-separated state is involved in the ICT process. As DMABN is the best studied example, we have performed calculations on the low-lying singlet and triplet states of the molecule along the twisting coordinte and also along the wagging coordinate to check the reliability of the proposed wagged-based model. In order to get more insight into the TICT problem, the *p*-aminobenzonitrile (ABN) molecule, in which no evidence of dual fluorescence was reported,[13,14,30] is also included in the present study (also benzonitrile was included for calibration purposes).

The complete active space (CAS) SCF approximation[47] in combination with a multiconfigurational second-order perturbation approach, the CASPT2 method,[48] and the use of high quality ANO-type basis sets has, in a number of earlier applications,[49-55] proven to be an efficient method for the calculation of the differential correlation effects on excitation energies. A multiconfigurational wave function is needed for the analysis of the properties of the excited states along the twisting coordinate. The CASPT2 method is used to obtain the corrections to the excitation energies, which are due to dynamic electron correlation effects, and which are of critical importance for obtaining quantitatively accurate results. Optimization of the geometries will be carried out on the molecules at the CASSCF level. The results give a theoretical basis for the understanding of the main features of the dual fluorescence and may direct further experimental studies on these and similar systems.

(36) Cowley, D. J.; Peoples, A. M. *J. Chem. Soc., Chem. Commun.* **1977**, 352.
(37) Rettig, W.; Bonacić-Kouteký, V. *Chem. Phys. Lett.* **1979**, *62*, 115.
(38) Lewis, F. D.; Holman, III, B. *J. Phys. Chem.* **1980**, *84*, 2326.
(39) Lipinski, J.; Chojnacki, H.; Grabowski, Z. R.; Rotkiewicz, K. *Chem. Phys. Lett.* **1980**, *70*, 449.
(40) LaFemina, J. P.; Duke, C. B.; Paton, A. *J. Chem. Phys.* **1987**, *87*, 2151.
(41) Majumdar, D.; Sen, R.; Bhattacharyya, K.; Bhattacharyya, P. *J. Phys. Chem.* **1991**, *95*, 4324.
(42) Khalil, O. S.; Meeks, J. L.; McGlynn, S. P. *Chem. Phys. Lett.* **1976**, *39*, 457.
(43) Kato, S.; Amatatsu, Y. *J. Chem. Phys.* **1990**, *92*, 7241.
(44) Cazeau-Dubroca, C.; Ait Lyazidi, S.; Cambeau, P.; Periqua, A.; Cazeau, Ph.; Pesquer, M. *J. Phys. Chem.* **1989**, *93*, 2347.
(45) Bhattacharyya, K.; Chowdhury, M. *Chem. Rev.* **1993**, *93*, 507.
(46) Bonacić-Kouteký, V.; Michl, J. *J. Am. Chem. Soc.* **1985**, *107*, 1765.
(47) See *e.g.*: Roos, B. O. In *Ab Initio Methods in Quantum Chemistry II*; Lawley, K. P., Ed.; J. Wiley & Sons Ltd.: 1987; p 399.
(48) Andersson, K.; Malmqvist, P.-Å.; Roos, B. O.; Sadlej, A. J.; Wolinski, K. *J. Phys. Chem.* **1990**, *94*, 5483. Andersson, K.; Malmqvist, P.-Å.; Roos, B. O. *J. Chem. Phys.* **1992**, *96*, 1218.
(49) Roos, B. O.; Andersson, K.; Fülscher, M. P. *Chem. Phys. Lett.* **1992**, *192*, 5. Fülscher, M. P.; Andersson, K.; Roos, B. O. *J. Phys. Chem.* **1992**, *96*, 9204.
(50) Serrano-Andrés, L.; Merchán, M.; Nebot-Gil, I.; Lindh, R.; Roos, B. O. *J. Chem. Phys.* **1993**, *98*, 3151. Serrano-Andrés, L.; Roos, B. O.; Merchán, M. *Theor. Chim. Acta* **1994**, *87*, 387.
(51) Serrano-Andrés, L.; Lindh, R.; Roos, B. O.; Merchán, M. *J. Phys. Chem.* **1993**, *97*, 9360.
(52) Rubio, M.; Merchán, M.; Ortí, E.; Roos, B. O. *Chem. Phys.* **1994**, *179*, 395.
(53) Serrano-Andrés, L.; Merchán, M.; Nebot-Gil, I.; Roos, B. O.; Fülscher, M. P. *J. Am. Chem. Soc.* **1993**, *115*, 6184. Roos, B. O.; Serrano-Andrés, L.; Merchán, M. *Pure Appl. Chem.* **1993**, *65*, 1693.
(54) Roos, B. O.; Merchán, M.; McDiarmid, R.; Xing, X. *J. Am. Chem. Soc.* **1993**, *116*, 5927.
(55) Serrano-Andrés, L.; Merchán, M.; Fülscher, M. P.; Roos, B. O. *Chem. Phys. Lett.* **1993**, *211*, 125.

2. Methods and Computational Details

The molecule was placed in the yz plane, with z as the long axis. Initially, multiconfigurational wave functions were determined at the CASSCF level of theory. The same space of active electrons and orbitals was used in both the geometry optimization procedure and the final calculations of the transition energies of the two molecules ABN and DMABN. It included the ten π electrons in the π system of the benzonitrile plane (yz) and the lone-pair electrons on the aniline-type nitrogen. The nine corresponding orbitals were active. The carbon and nitrogen 1s electrons were kept frozen in the final calculations in the form determined by the ground state SCF wave function and were not included in the calculation of the correlation energy. All remaining orbitals were inactive, along with the π_y orbital of the CN group perpendicular to the π system of the ring. The old suggestion[16] about the role of this orbital in the charge transfer mechanism was ruled out a long time ago,[42] which is also confirmed here. Electronic states involving excitations from bonding or to antibonding orbitals with a dominating π-CN character have been shown to lie at high energies, both by previous results[39,42] and results obtained here with a minimal basis set. Thus, the excitations included in the CAS configuration space were of $\pi-\pi^*$ and $n-\pi^*$ character, while no excitations out of the σ or π_y orbitals were considered. Dipole moments and population analysis data were computed at the CASSCF level. The CASSCF interaction method (CASSI)[56] was used to compute oscillator strengths using energy differences corrected for by CASPT2. The CASPT2 method[48] calculates the first-order wave function and the second-order energy in the full-CI space without any further approximation, with a CASSCF wave function constituting the reference function. The approach where the full Fock matrix is employed in the definition of the zeroth-order Hamiltonian (PT2F) was used.

Geneally contracted basis sets of the atomic natural orbital (ANO) type[57,58] were used, which were obtained from N,C(10s6p3d)/H(4s) primitive sets. The contraction used,[59] N,C[3s2p1d]/H[2s], has been shown to be flexible enough for the description of the valence excited states of a system as larger as naphthalene.[52] It has also been shown to be the smallest one, which gives reliable results, among a series of basis sets tested for the calculation of the excitation energies in the pyrazine molecule.[60]

The calculations were performed in four steps. First, the ground state geometries of ABN and DMABN were optimized at the CASSCF level of theory, using a DZP quality basis set.[61] No spatial symmetry restrictions were used in the ground state optimizations. In ABN, the optimized geometry turned out to have C_{2v} symmetry with a planar amino group. The geometry of the optimized DMABN ground state belonged to the C_s symmetry, with the amino group bent out of the plane. In the second step vertical excitation energies for the two lowest singlet and triplet states were computed using the CASSCF/CASPT2 approach and the ANO basis sets. Actual calculations were performed in C_1 symmetry. State average calculations were carried out for the three singlet states (the ground state, the LE, and the CT state) and the two triplet states, respectively. The calculations of the second step were repeated for the twisting angles 30, 60, and 90°. Two sets of calculations were performed for both molecules: one with the N-inversion angle set to zero and the other using the angle 21°; which is the optimal value for the ground state in DMABN, and it is used here as an estimation in ABN. In addition, calculations were performed of the three singlet states at a nontwisted geometry and along the wagging coordinate (0, 10, 21, 34 and 45° as wagging angle in ABN and 0, 10, 21, 30, and 40° in DMABN). It might be worth mentioning that the DMABN calculations are among the largest performed with the MOLCAS system. The size of the basis set is 174, and no spatial symmetry is available to reduce the computational effort. Founded on our earlier experience with these type of calculations we expect the excitation energies to carry errors not larger than 0.3 eV.

The calculations have been performed on an IBM RS/6000 workstation (Model 580) at the University of Valencia, using the MOLCAS-2[62] and the preliminary MOLCAS-3[63] quantum-chemistry software, which includes as different modules the CASPT2 and the ALASKA (SCF and CASSCF gradient code)[64] programs.

Table 1. Ground State Geometries of ABN and DMABN[a]

	ABN		DMABN			
	CAS[c]	expl[d]	SCF[e]	CAS[c]	expl[d]	exp2[f]
			Bonds[b]			
N_1C_1	1.367	1.370	1.446	1.388	1.367	1.379
C_1C_2	1.399	1.405	1.402	1.406	1.400	
C_2C_3	1.391	1.369	1.379	1.391	1.370	
C_3C_4	1.399	1.398	1.394	1.399	1.388	
C_4C_5	1.446	1.431	1.458	1.446	1.434	1.454
C_5N_2	1.158	1.148	1.157	1.157	1.145	
C_2H_1	1.078		1.078	1.072		
C_3H_2	1.076		1.084	1.076		
N_1C_6			1.486	1.460	1.456	
C_6H_3			1.093	1.095		
C_6H_4			1.087	1.087		
C_6H_5			1.088	1.082		
N_1H_3	0.989	0.900				
			Angles[g]			
$N_1C_1C_2$	120.8		121.5	121.3		
$C_1C_2C_3$	120.9		121.1	121.4		
$C_2C_3C_4$	120.4		120.8	120.6		
$C_4C_5N_2$	180.0		180.0	180.0		
$C_1C_2H_1$	119.6		120.7	120.6		
$C_4C_3H_2$	119.9		119.7	120.0		
$C_1N_1H_3$	120.8	115.0				
$C_6N_1C_6$			115.1	115.6	116.4	115.7
$C_1N_1C_6$			122.4	122.2	121.6	
$N_1C_6H_3$			112.4	113.5		
$N_1C_6H_4$			111.3	111.1		
$N_1C_6H_5$			108.1	109.5		
			Dihedral Angles[g]			
$C_2C_1N_1C_6$			41.8	21.2	11.9	15
$C_1N_1C_6H_3$			60.4	57.7		
$C_1N_1C_6H_4$			61.2	65.3		
$C_1N_1C_6H_5$			189.5	177.5		
$C_2C_1N_1H_3$		34				

[a] ABN, C_{2v} symmetry; DMABN, C_s symmetry. See text and Figure 1. [b] See Figure 1 for atom labeling. Distances in Å. [c] Present CASSCF results using a DZP[61] quality basis set. [d] Crystal X-ray structure.[66] [e] SCF results using a STO-3G minimal basis set from ref 43. [f] Estimated value from microwave spectroscopy data: ref 65. [g] Valence and dihedral angles in deg.

3. Results

3.1. The Geometries of the Ground States of ABN and DMABN. The ground state geometries of ABN and DMABN were optimized at the CASSCF level of theory. Table 1 shows the computed geometries and the comparison with available experimental data[65,66] (cf. Figure 1 for atom numbering). The out-of-plane wagging angle of the amino group in DMABN is computed to be 21.2°, near the experimental estimate of 15° [65]

(56) Malmqvist, P.Å. *Int. J. Quantum Chem.* **1986**, *30*, 479. Malmqvist, P.-Å.; Roos, B. O. *Chem. Phys. Lett.* **1992**, *155*, 189.
(57) Almlöf, J.; Taylor, P. R. *J. Chem. Phys.* **1987**, *86*, 4070.
(58) Widmark, P.-O.; Malmqvist, P.-Å.; Roos, B. O. *Theor. Chim. Acta* **1990**, *77*, 291.
(59) Pierloot, K.; Dumez, B.; Widmark, P.-O.; Roos, B. O. *Theor. Chim. Acta* **1995**, *90*, 87. Pou-Amérigo, R. for H basis set, private communication.
(60) Fülscher, M. P.; Roos, B. O. *Theor. Chim. Acta* **1994**, *87*, 403.
(61) Dunning, T. H.; Hay, P. J. In *Modern Theoretical Chemistry*; Plenum Press: New York, 1976; p 1.
(62) Andersson, K.; Blomberg, M. R. A.; Fülscher, M. P.; Kellö, V.; Lindh, R.; Malmqvist, P.-Å.; Noga, J.; Olsen, J.; Roos, B. O.; Sadlej, A. J.; Siegbahn, P. E. M.; Urban, M.; Widmark, P.-O. MOLCAS, Version 2; University of Lund, Sweden, 1991.
(63) MOLCAS-3 is an experimental extension of the quantum chemistry package MOLCAS-2.
(64) Lindh, R.; Ryu, U.; Liu, B. *J. Chem. Phys.* **1991**, *95*, 5889. Lindh, R. *Theor. Chim. Acta* **1993**, *423*, 85.
(65) Kajimoto, O.; Yokohama, H.; Ooshima, Y.; Endo, Y. *Chem. Phys. Lett.* **1991**, *179*, 455.
(66) Heine, A.; Herbst-Irmer, R.; Stalke, D.; Kühnle, W.; Zachariasse, K. A. *Acta Crystallogr.* in press.

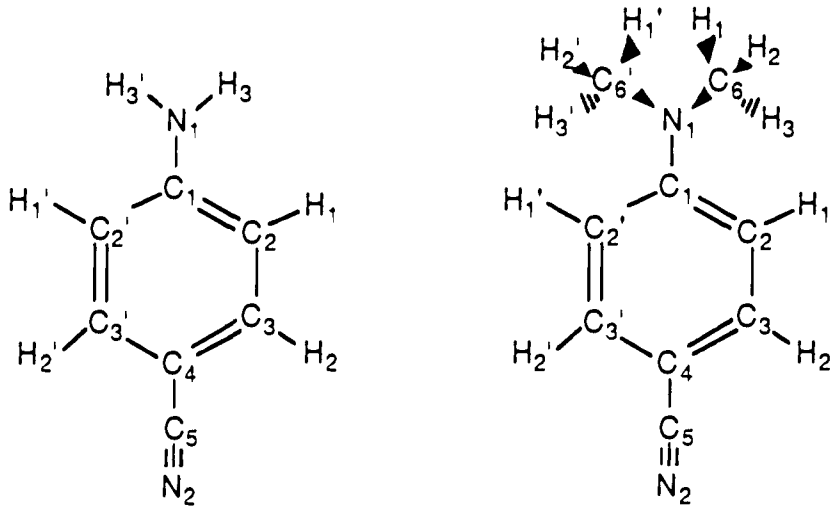

Figure 1. *p*-Aminobenzonitrile (ABN) and (*p*-dimethylamino)benzonitrile (DMABN) atom labels. ABN, C_{2v} symmetry and DMABN, C_s symmetry, with z as the main symmetry axis.

and 11.9°.[66] The computed bond distances deviate from microwave data with at most 0.009 Å for the few distances that have been measured. The deviations from the crystal data[66] are somewhat larger, although within the limit of 0.02 Å. Some uncertainty, mainly in the tilt angle, should be assumed in the microwave data due to the approximations included to fit the obtained spectra. Our CASSCF results agree with the general finding in aminobenzonitriles, where the C_1-C_2 bond is the longest in the benzene ring while the C_2-C_3 is the shortest.[67] For comparison, microwave measurements in benzonitrile obtained the distances: 1.391 Å (C_1-C_2), 1.393 Å (C_2-C_3), and 1.400 Å (C_3-C_4),[68] As expected, the distance in ABN and DMABN, which is most affected by the substituent effect is the C_1-C_2 bond. The central (C_2-C_3) phenyl bond in DMABN (1.391 Å) is computed to be 0.02 Å longer than the X-ray result (1.370 Å). It has, however, been observed that solid-phase X-ray measurements sometimes underestimate the length of bonds of this type by around 0.02 Å,[51,69] An argument is put forward in ref 66, which explains the observed double bond character in the central CC bond as being due to the appearance of ionic structures in the wave function. However, such an explanation would also inevitably lead to elongations of the C_1-C_3 and C_3-C_4 bonds, which is not observed. We conclude that the measured C_2-C_3 bond length is too short.

Included in Table 1 are also the results from an SCF optimization of DMABN obtained with an STO-3G basis set.[43] The resulting bond distances are very similar to those obtained here, with one notable exception, the amino–carbon bond, where the SCF result is 0.067 Å too long. Also the wagging angle is grossly overestimated at the SCF (STO-3G) level of theory (42° instead of 21°).

The CASSCF results have been obtained without using any spatial symmetry in the calculations. ABN comes out as a planar system with C_{2v} symmetry. Crystal X-ray measurements[66] point out, however, that the ABN molecule is actually wagged by around 34° in its ground state. Intermolecular hydrogen bonds were detected which might affect the wagging angle. A more clear measurement of the wagging angle should come from a technique where the hydrogen atoms were located with accuracy, like neutron scattering. Nevertheless, this finding is consistent with the gas-phase wagging angle in aniline, reported around 40°,[70] The fact that the CASSCF calculation lead to a planar molecule can be related to the limited active space employed, which only comprises the π system over the benzonitrile plane. Strong delocalization of the charge over the nitrogen and the benzonitrile moiety trends to favor a planar conformation. To check the evidence of a wagged ground state in ABN we performed calculations for the ground state at the CASPTP2 level, scanning the wagging angle from 0 to 60°. Around an angle of 17° an energy minimum was obtained. The study of the twisting process in ABN has been performed both for fixed wagging angles of 0 and 21°. The latter angle was selected as an estimate, to compare the potential energy curve in both molecules and because of the 21° wagged angle is near the CASPT2 computation for the ground state minimum. DMABN, on the other hand, has the amino group bent out of the plane at the CASSCF level of theory at 21.2°. The more detailed study of the effect of the wagging angle on the energy of DMABN described in section 3.3 gives an energy minimum for the ground state at around 10° at the CASPT2 level, which is consistent with the 11.9° obtained by the X-ray measurements.[66] The CASPT2 barrier to planarity (using the ANO basis set) was found to be around 3 kcal/mol. This is only an approximation to the actual gas-phase value, since the geometry was not fully optimized at the CASPT2 level of theory. In order to analyze the influence of the tilting angle, the twisting process for both molecules has been studied at two wagging angles: 0 and 21°. Furthermore, the influence of the wagging angle in the low-lying singlet states at the nontwisted geometry will be considered in both systems.

3.2. The Excited States of ABN and DMABN—a Qualitative Analysis. The ground and low-lying valence singlet and triplet states have been studied at the optimized geometries for the ground states of the molecules ABN and DMABN and at the geometries resulting from twisting the amino group by 30, 60, and 90° with respect to the benzonitrile moiety. The goal is to study the energies and properties of these states along the twisting coordinate. In this section we discuss the qualitative features of the wave functions for the twisting angles 0 and 90°.

The nine valence π-orbitals included in the calculations are those forming the out-of-plane π system in the ground state

(67) Merlino, S.; Sartori, F. *Acta Cryst.* **1982**, *B38*, 1476.
(68) Bak, B.; Christensen, D.; Dixon, W. B.; Hansen-Nygaard, L.; Rastrup-Andersen, *J. Chem. Phys.* **1994**, *37*, 2027.
(69) Baughman, R. H.; Kohler, B. E.; Levy, I. J.; Spangler, C. *Synth. Met.* **1985**, *11*, 37. Hamilton, T. P.; Pulay, P. *J. Phys. Chem.* **1989**, *93*, 2341.
(70) Quack, M.; Stockburger, M. *J. Mol. Spectrosc.* **1972**, *43*, 87. Lister, D. G.; Tyler, J. K.; Hog, J. H.; Wessel-Larsen, N. *J. Mol. Struct.* **1974**, *23*, 253.

Table 2. SCF Orbital Energies for ABN, DMABN, and BzCN (Benzonitrile) and CASSCF Configuration Weights for the Low-Lying Singlet States of ABN and DMABN at Nontwisted and 90° Twisted Conformations

	ABN		DMABN		BzCN[a]
	nontwisted	twisted	nontwisted	twisted	nontwisted
SCF total energies (au)	−377.494 039	−377.471 743 2	−455.541 197	−455.531 040	−322.457 252
			SCF Orbital Energies (eV)[b]		
$\epsilon_1[1pN_b]$	−12.11	−10.99	−11.51	−10.04	
$\epsilon_2[\pi_{r,a}]$	−9.93	−10.14	−9.86	−9.87	−9.97
$\epsilon_3[\pi_{r,b}]$	−8.51	−9.38	−8.46	−9.54	−9.83
$\epsilon_4[\pi^*_{r,b}]$	2.54	1.65	2.45	1.92	1.76
$\epsilon_5[\pi^*_{r,a}]$	2.69	2.74	2.78	2.72	2.58
			SCF Energy Differences (eV):[b] b Symmetry		
$\epsilon_5[\pi^*_{r,a}]-\epsilon_1[1pN_b]$	14.80	13.73	14.29	12.76	
$\epsilon_4[\pi^*_{r,b}]-\epsilon_2[\pi_{r,a}]$	12.47	11.79	12.31	11.79	11.73
$\epsilon_5[\pi^*_{r,a}]-\epsilon_3[\pi_{r,b}]$	11.20	12.12	11.24	12.26	12.41
			SCF Energy Differences (eV):[b] a Symmetry		
$\epsilon_4[\pi^*_{r,b}]-\epsilon_1[1_pN_b]$	14.65	12.64	13.96	11.96	
$\epsilon_5[\pi^*_{r,a}]-\epsilon_2[\pi_{r,a}]$	12.62	12.88	12.64	12.59	12.55
$\epsilon_4[\pi^*_{r,b}]-\epsilon_3[\pi_{r,b}]$	11.05	11.03	10.91	11.46	11.59
			Contributions to the Wave Function from Different Types of Excitations:[b,c] 1^1B State		
$\pi_{r,b}-\pi^*_{r,a}$	51.4	33.9	44.7	29.7	
$\pi_{r,a}-\pi^*_{r,b}$	24.5	41.0	30.9	46.5	
$1pN_b-\pi^*_{r,a}$	0.0	0.0	0.0	2.2	
oth.single.	1.3	0.3	2.0	0.0	
doubles	14.4	16.1	13.1	16.2	
higher	0.3	4.0	0.8	2.2	
			Contributions to the Wave Function from Different Types of Excitations:[b,c] 2^1A State		
$\pi_{r,b}-\pi^*_{r,b}$	71.4	0.0	75.1	1.9	
$\pi_{r,a}-\pi^*_{r,a}$	1.9	0.0	3.5	0.0	
$1pN_b-\pi^*_{r,b}$	0.9	83.4	1.2	87.7	
oth single.	6.6	0.0	2.0	0.0	
doubles	9.0	10.1	6.9	2.8	
higher	1.7	2.6	2.4	4.1	

[a] For BzCN the optimized geometry of ABN was used. [b] Label r indicates an orbital of the ring (benzonitrile moiety). Labels a, b denote the symmetry. [c] Weights (in %) of all configurations with coefficients larger than 0.05.

CASSCF minimum conformation, *i.e.*, without any twisting. This active space includes the benzene ring π ($\pi_{r,b}$, $\pi_{r,a}$) and π^* ($\pi^*_{r,b}$, $\pi^*_{r,a}$) orbitals, the π_x and π^*_x orbitals of the CN group, and the lone-pair orbital on the aniline-type nitrogen (lpN). Label r indicates an orbital of the ring (benzonitrile moiety). Labels a, b denote the symmetry. Table 2 presents the energies and energy differences for the highest occupied and lowest empty SCF orbitals for ABN, DMABN, and benzonitrile (BzCN). The label of the orbitals should be considered with caution, because of the strong mixing occurring among the π orbitals of b symmetry (C_2 framework). This is most prominent for ABN in the planar geometry, where all orbitals are delocalized over the entire π system.

Let us for a moment assume that the relative energies are related to orbital energy differences. As expected, the most striking change in the orbital energies in going from the nontwisted to the 90° twisted conformation is the destabilization of the lone-pair orbital, while the HOMO (π_{ring}) and LUMO (π^*_{ring}) orbitals stabilize. The lone-pair orbital is delocalized over the entire π system at the parallel conformation but not in the perpendicular situation, where the symmetry forces it to be localized. At the 90° twisted conformation the orbital energies of the ring π orbitals are also very similar to those of the BzCN molecule. Thus, changes on twisting should be expected in the energies of states with important contributions of excitations from the lpN and $\pi_{r,b}$ orbitals to the $\pi^*_{r,b}$ orbital. The SCF energy differences on Table 2 suggest that the most important change due to the twisting will be on the state of A symmetry, where the orbital energy difference $\pi^*_{r,b}-1pN$ is strongly decreased, while the other differences are maintained. The states of B symmetry will not be affected to the same extent. Here one orbital energy difference increases while the other decreases. The effect is stronger in DMABN than it is in ABN.

At nontwisted geometries the lone-pair orbital is 0.5 eV more stable in ABN, and the difference increases to 1 eV in the twisted form. Increasing the size of the alkyl chain will lower the ionization potential for the lone-pair, since the substituents become more polarizable, which stabilizes states where the nitrogen atom is charged (ionic or CT states). The ionization potentials (IP) decrease in the series $MeNH_2$, Me_2NH, and Me_3N: 8.89 eV, 8.15 eV, and 7.76 eV,[71] respectively. A result is the increased importance of dual fluorescence in molecules where the substituent on the nitrogen is a larger alkyl chain as in diethylamine.[30] The IP for the ethylamines $EtNH_2$, Et_2NH, and Et_3N are 8.76, 7.85, and 7.11 eV, respectively,[71] which is lower than the methylamines potentials. The charge transfer takes place easier in molecules with long, more polarizable, chains attached to the nitrogen atom. The same trend is found when the oxidation potential of the isolated amino group is measured in the molecules ABN, MABN (*p*-methylamino)-benzonitrile), and DMABN,[13] although the oxidation potential of trialkylamines becomes practically constant after ethyl, while the ICT rate constant still increases.[30]

The relation between the ionization potential and the mobility of the charge with the rate constant comes through the energy barrier in the potential energy curve. Increasing the alkyl chain on the nitrogen means (Table 2) a less stable lone-pair orbital due to the polarizability of the substituent and this leads to a

(71) Aue, D. H.; Webb, H. M.; Bowers, M. T. *J. Am. Chem. Soc.* **1976**, *98*, 311.

Table 3. Computed Energies (ΔE),[a] Oscillator Strengths[b] (*f*), and Dipole Moments[c] (μ) of the Electronic States of ABN and DMABN at Several Geometries along the Twisting Coordinate (θ)[d]

	θ = 0 deg			θ = 30 deg			θ = 60 deg			θ = 90 deg		
state	ΔE	*f*	μ	ΔE	*f*	μ	ΔE	*f*	μ	ΔE	*f*	μ
					p-Aminobenzonitrile (ABN): 0° Wagging Angle							
1^1A			6.89			6.58			5.83			5.51
1^1B	4.01	0.004	6.70	4.02	0.081	6.87	3.99	0.018	5.19	4.24	0.002	5.21
2^1A	4.44	0.361	12.42	4.45	0.324	12.83	4.49	0.099	13.01	3.82	0.000	15.75
1^3A	3.37		6.19	3.29		6.72	3.13		5.73	3.25		5.64
1^3B	3.88		7.74	4.04		7.26	4.20		5.35	4.11		5.82
					p-Aminobenzonitrile (ABN): 21° Wagging Angle							
1^1A			6.30			6.23			5.27			4.86
1^1B	4.17	0.002	6.06	4.29	0.001	6.03	4.37	0.002	5.04	4.10	0.007	4.65
2^1A	4.54	0.358	12.08	4.59	0.331	12.00	4.35	0.207	12.81	4.54	0.000	15.65
1^3A	3.92		6.17	3.41		5.99	3.19		5.39	3.12		5.02
1^3B	3.93		6.89	4.16		6.47	4.23		5.43	3.96		5.26
					(*p*-Dimethylamino)benzonitrile (DMABN): 0° Wagging Angle							
1^1A			7.36			6.84			6.04			5.75
1^1B	4.05	0.010	7.58	3.99	0.004	6.99	4.30	0.001	6.13	4.55	0.003	5.70
2^1A	4.41	0.416	13.79	4.17	0.200	13.58	3.97	0.033	14.63	3.94	0.000	15.61
1^3A	3.66		6.84	3.58		6.90	3.64		6.00	3.65		5.56
1^3B	3.69		10.39	3.63		9.27	4.20		6.41	4.40		5.92
					(*p*-Dimethylamino)benzonitrile (DMABN): 21° Wagging Angle							
1^1A			6.40			6.37			5.47			5.10
1^1B	4.02	0.003	6.33	4.18	0.004	6.35	4.40	0.003	5.40	4.58	0.006	4.87
2^1A	4.23	0.411	13.27	4.13	0.308	13.23	3.85	0.112	14.58	3.74	0.000	15.45
1^3A	3.50		6.33	3.63		6.25	3.85		5.44	3.92		5.17
1^3B	3.80		7.61	4.16		6.93	4.53		5.64	4.56		5.50

[a] Energies at the CASPT2 level (eV). [b] Oscillator strengths computed with CASSCF transition moments and CASPT2 energies. [c] Dipole moments at the CASSCF level (D). [d] See Figures 2 and 3.

lower "true" lone-pair (lpN) → LUMO state (see below). As the behavior of the 2^1A state and even the 1^1B state potential energy curves depends on the avoided crossing between the lpN → LUMO and the HOMO → LUMO states, the trends on activation energies and rate constants on increasing the alkyl chains can be understood. When the energy difference between the ^1A "true" lone-pair (lpN) → LUMO state and the 1^1B and 2^1A states decreases at the nontwisted geometry, the crossing of the potential energy surfaces will take place at smaller twisting angles resulting in lower barriers.

The situation is reflected in the structure of the CASSCF wave functions for the low-lying excited singlet states for ABN and DMABN (cf. Table 2). The 1^1B state is a typical minus state (1^1B^-) with dominant contributions from the HOMO → LUMO + 1 and HOMO − 1 → LUMO single excitations. As is typical for these type of excited states in conjugate π systems,[55] there are important contributions from di-excited configurations. Both for ABN and DMABN, twisting to the perpendicular conformation does not lead to great changes in the structure of the state, except that the weights of the involved configurations interchange, as the SCF orbital energy differences suggested. The importance of the lone-pair orbital is higher in the A state. The 2^1A state is dominated by a singly excited configuration. At the nontwisted geometry the wave function is mainly composed of the HOMO → LUMO excitation, although it should be noted that the HOMO orbital includes a strong mixing with the lone-pair orbital. Thus, the excitation lpN → $\pi^*_{r,b}$, the most important for the 2^1A state at the twisted form (83.4% of the CASSCF wave function in ABN, 87.7% in DMABN), is to some extent included also in the nontwisted wave function. As a consequence, some of the charge transfer inferred by the n → π* transition is included already in the 2^1A state in the nontwisted conformation due to the overlap of the orbitals, although it is not the CT state observed in the fluorescence spectrum. The nature of the S_2 state explains the experimental evidence that the pure CT state cannot be reached by direct absorption from the ground state.[13,34] The state is present in emission but only after the isomerization. No qualitative difference between the molecules is observed by inspection of the wave function. From this point of view the structure of the states is formally the same for ABN and DMABN. Using a wagged geometry in ABN, a slight stabilization of the lone-pair orbital is achieved: 0.13 and 0.25 eV at the nontwisted and twisted geometries, respectively. Within this simple model, no significant changes in the description of the corresponding excited states involving the orbital are therefore expected.

3.3. The Ground State, LE, and CT Potential Curves for ABN and DMABN. The results obtained for excitation energies, dipole moments, and oscillator strengths for ABN and DMABN along the twisting coordinate with two wagging angles (0 and 21°) are presented in Table 3. Table 4 presents the effective charges located on the different moieties for the computed states at the nontwisted and twisted geometries. Table 5 presents the energies, oscillator strengths, dipole moments, and effective charges computed for the lowest singlet states of nontwisted ABN and DMABN along the wagging coordinate. The corresponding potential curves are given in Figures 2–4. All the transition energies reported along this paper are vertical energies, *i.e.*, they have been calculated, unless some other procedure is specified, as the difference between the excited state energy and the energy of the ground state, using the same geometry for both.

Inspection of the potential curves along the twisting path shows that the ground and 1^1B states have minima at nontwisted and maxima at perpendicular geometries in both molecules. The potential curve for the 2^1A state has different shapes in the two systems. In the nonwagged ABN (cf. Figure 2, wg0) it has two minima, one at the planar geometry and another at the twisted conformation. At around 60° there is a barrier of 0.36 eV separating the two minima. The minimum at 90° is 0.25

Table 4. Effective Charge Distribution[a] in the Ground (GS) and Lowest Electronic Singlet and Triplet Excited States of ABN and DMABN at Planar (θ = 0 deg) and Twisted (θ = 90 deg) Conformations

	ABN, nontwisted, wag, 0°					ABN, twisted, wag, 0°				
gr	GS	1^1B	2^1A	1^3A	1^3B	GS	1^1B	2^1A	1^3A	1^3B
NH_2	−0.018	0.029	0.228	−0.023	0.088	−0.111	−0.123	0.692	−0.166	−0.150
Bz	0.196	0.151	0.006	0.209	0.043	0.277	0.305	−0.488	0.327	0.328
CN	−0.178	−0.180	−0.234	−0.186	−0.131	−0.166	−0.182	−0.204	−0.161	−0.178
	ABN, nontwisted, wag, 21°					ABN, twisted, wag, 21°				
gr	GS	1^1B	2^1A	1^3A	1^3B	GS	1^1B	2^1A	1^3A	1^3B
NH_2	−0.023	0.004	0.199	−0.012	0.045	−0.207	−0.215	0.670	−0.151	−0.149
Bz	0.199	0.176	0.048	0.184	0.107	0.368	0.389	−0.473	0.311	0.318
CN	−0.175	−0.180	−0.247	−0.172	−0.152	−0.161	−0.174	−0.197	−0.160	−0.169
	DMABN, nontwisted, wag, 0°					DMABN, twisted, wag, 0°				
gr	GS	1^1B	2^1A	1^3A	1^3B	GS	1^1B	2^1A	1^3A	1^3B
NMe_2	−0.022	0.050	0.309	−0.019	0.203	−0.087	−0.097	0.582	−0.098	−0.092
Bz	0.207	0.129	−0.065	0.202	−0.042	0.263	0.278	−0.346	0.272	0.287
CN	−0.185	−0.179	−0.244	−0.183	−0.161	−0.176	−0.181	−0.236	−0.175	−0.195
	DMABN, nontwisted, wag 21°					DMABN, twisted, wag, 21°				
gr	GS	1^1B	2^1A	1^3A	1^3B	GS	1^1B	2^1A	1^3A	1^3B
NMe_2	−0.036	−0.007	0.256	−0.030	0.070	−0.167	−0.177	0.660	−0.096	−0.093
Bz	0.197	0.164	0.002	0.195	0.063	0.317	0.339	−0.435	0.246	0.257
CN	−0.161	−0.157	−0.258	−0.165	−0.133	−0.150	−0.162	−0.225	−0.150	−0.164

[a] CASSCF (10 electrons−9 orbitals) calculations.

eV lower in energy than that occurring at the planar conformation. This situation is characteristic of an avoided crossing between states of different nature and can be understood from the structure of the wave function. The 21° wagged ABN (cf. Figure 2, wg21) presents a similar behavior, with a destabilization of the 2^1A state along the twisting coordinate. The energy increases around 0.10 eV in going to a twist angle of 60°, which is lower than for the nonwagged form. At a 90° twisted conformation the energy is now higher. At the nontwisted geometry the 2^1A state is mainly described by the single excitation $\pi_{r,b} \rightarrow \pi^*_{r,b}$ (HOMO → LUMO), where the contribution of the lone-pair orbital is made through the delocalized nature of the HOMO and LUMO orbitals over the benzene plane. At the twisted geometry the 2^1A state is also characterized by a singly excited configuration from the lone-pair orbital (lpN) to the LUMO ($\pi^*_{r,b}$) orbital, with the latter now completely localized to the benzonitrile moiety. In order to obtain a more detailed view of this structure, calculations were performed on the ABN 3^1A state at the twisted conformation. This state, for the nonwagged molecule, presents a computed excitation energy of 5.81 eV and a dipole moment of 3.54 D, and it corresponds mainly to the HOMO → LUMO one-electron promotion (coefficient 0.8) between orbitals entirely located on the benzonitrile moiety. In the wagged ABN the 3^1A state at the twisted geometry stabilizes to 4.97 eV, 0.42 eV above the CT state. In the 21° wagged DMABN (cf. Figure 3, wg21) the energy of the 2^1A state decreases along the twisting coordinate with a minimum at the 90° twisted geometry, 0.39 eV below the nontwisted conformation. In the nonwagged DMABN (cf. Figure 3, wg0), the state stabilizes by 0.08 eV at 60° of twisting, while the perpendicular conformation presents a local maxima only 0.02 eV lower than the nontwisted geometry. In DMABN the rotation barrier in the 2^1A state disappears due to the stabilization of the CT configuration already near the nontwisted conformation. It is possible that the barrier in ABN can be decreased somewhat by also optimizing the wagging angle. The qualitative difference between the two energy surfaces will, however, remain. The rotation barriers in the 2^1A state are not the activation barriers for the ICT reaction because of the reaction that will take place in the surface obtained by coupling the 1^1B and 2^1A states. It should also be noted that the crossing between the A and B state potential curves in the calculations with the 21° wagged amino groups is actually avoided since the states now belong to the same symmetry (Figures 2 and 3, wg21). Here we have used the labels S_1 and S_2 to represent the resulting states. The shape of the curves should be a good approximation to the reaction paths for the photophysical reactions in both molecules. Near the ground state nontwisted conformations, the gap between the singlet excited states is smaller in the DMABN system than the ABN molecule.

The computed oscillator strengths and dipole moments for the different states (cf. Table 3) illustrate the different nature of them. The ground state dipole moments in the non-twisted form for the two molecules are very similar in magnitude. They continuously decrease with increasing twist angle. The dipole moments of the 1^1B states are even lower than those of the ground states (except in the nonwagged DMABN), and they also decrease along the twisting coordinate (except in ABN where there is first a small increase). All oscillator strengths corresponding to excitation to the 1^1B state are very small. The 2^1A state behaves differently. The dipole moment is large already in the non-twisted conformation (12.00 D for ABN and 13.27 D for DMABN) and is very similar in the wagged and nonwagged conformation. At 60 and 90° the dipole moment increases considerably. Thus, a strong interaction with the solvent is expected in the 2^1A state, which should be reflected in the transition energy of both the absorption and the fluorescence spectra. The oscillator strengths clearly reflect the change in the nature of the 2^1A state. While the values for the nontwisted situation are 0.356 and 0.411 for wagged ABN and DMABN, respectively, illustrating their Franck−Condon allowed character, the intensity decreases along the twist coordinate and becomes zero at the perpendicular conformation where the excitation is a forbidden n → π^* transition.

The computed energies of the electronic states show the importance of the wagging angle in the 2^1A excited state, although the behavior is completely different in ABN and DMABN, undoubtedly due to the interaction of the lone-pair

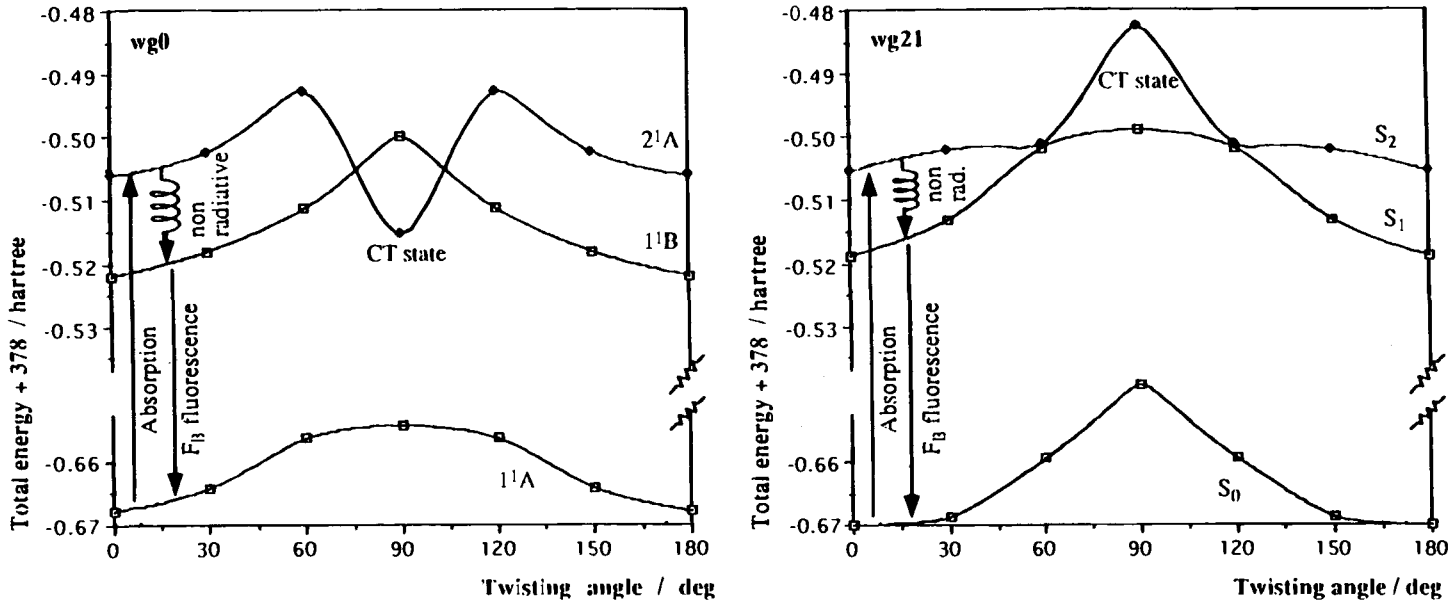

Figure 2. Ground and low-lying singlet excited states potential curves in ABN along the twisting coordinate. The amino groupo is wagged by 0° (wg0) or 21° (wg21).

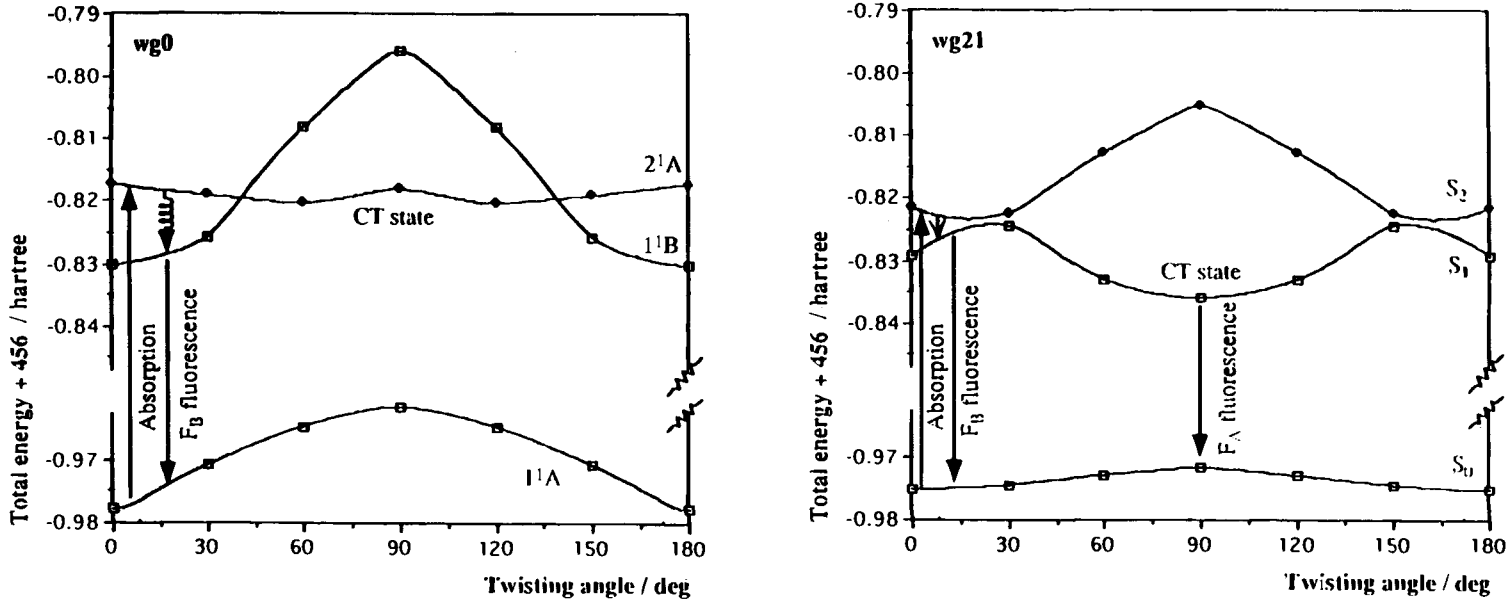

Figure 3. Ground and low-lying singlet excited states potential curves in DMABN along the twisting coordinate. The dimethylamino group is wagged by 0° (wg0) or 21° (wg21).

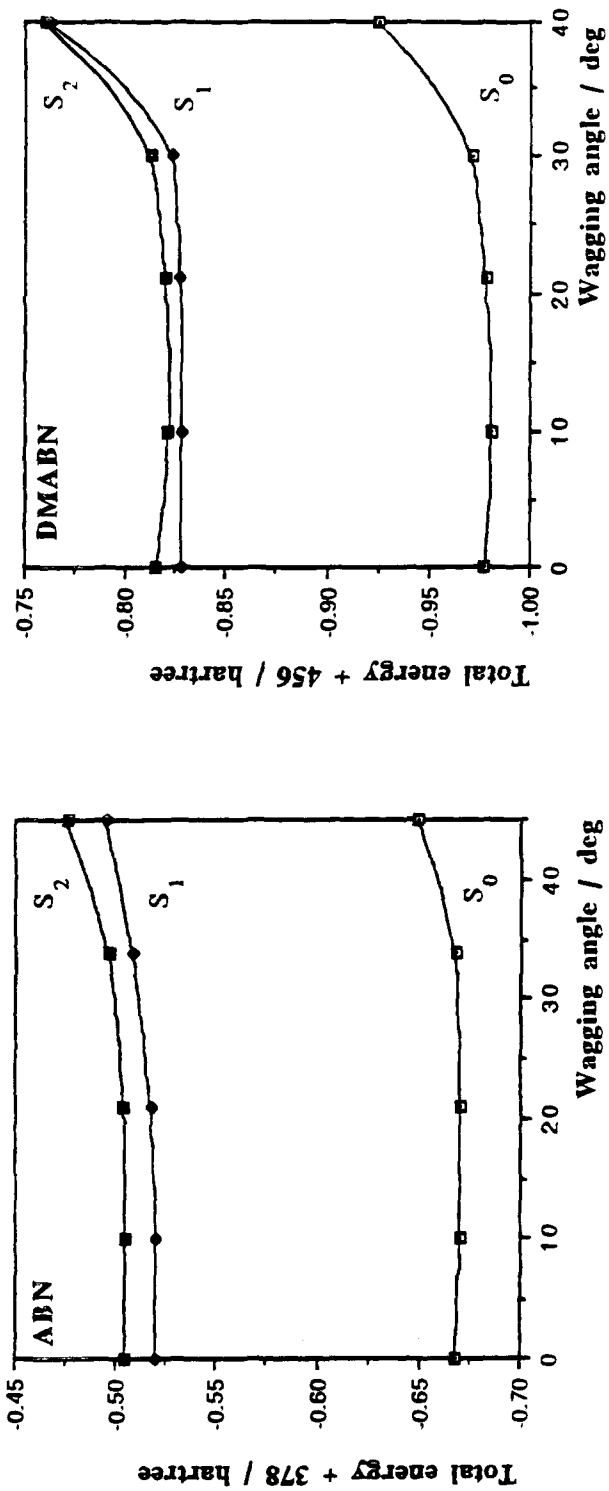

Figure 4. Ground and low-lying singlet excited states potential curves in ABN and DMABN along the wagging coordinate. The amino groups are not twisted.

electrons with the substituents on the nitrogen. In ABN, the energy of the conformation with a wagging angle of 21° is lower than that of the nonwagged form, except at the perpendicular conformation, where the energy is 0.89 eV lower in the nonwagged form. The barrier in the twist coordinate around 60° is 0.36 eV in the nonwagged form. This barrier must, however, be considerably lower along the minimum energy path, since the cost to twist the NH_2 group to 60° is only about 0.10 eV in the wagged geometry. In DMABN the wagged form is the more stable conformation at all the computed twisting geometries. The inversion barrier varies along the twisting path from 0.1 eV at the nontwisted form to 0.4 eV at the 90° geometry.

The excitation energy of the 1^1B state in both molecules is not significantly affected by the wagging angle. The state comprises excitations mostly within the benzonitrile moiety (cf. Table 2). In ABN the 1^1B state is about 0.1−0.2 eV more stable in the nonwagged form along the twisting coordinate. In DMABN the nonwagged 1^1B state is less than 0.1 eV more stable in the nonwagged conformation at 0 and 30° of twisting, and 0.13 and 0.25 eV more stable in the wagged conformation at the twist angles 60° and 90°. The potential curve for the B state is very flat up to a twisting angle of 30°. The calculated energy difference is less than 0.1 eV in all the cases studied. Actually, the equilibrium geometry of this state has been estimated by microwave spectroscopy to correspond to a twist angle of about 30° and no wagging angle.[65] Since the geometry of this state has not been optimized here, we cannot confirm or rule out the structure suggested by the experiment. It is, however, clear that the system is very flexible in the 1^1B state around the nontwisted geometry. A minimum in the 1^1B state at a twisting angle of around 30° has been used by some authors[35,72,73] as an argument against the relationship between twisting and dual fluorescence. The twisting to the perpendicular CT state takes place, however, on the S_1 surface, which after 30° of twisting, progressively increases its charge transfer character yielding a state with a different nature (the CT state) than the nontwisted S_1 state (nonpolar LE state). We also note that the closeness in energy of the strongly polar 2^1A state and the less polar 1^1B state makes a shift of the ordering, also close to the non-twisted geometries, plausible in similar systems as (*p*-dimethylamino)benzoic acid ethyl ester, where the two fluorescence bands seems to present long-axis polarization, that is, both fluorescences originate from the 2^1A state.[18]

Finally, the inspection of the computed effective charges on the different moieties (cf. Table 4) illustrates the charge transfer process occurring in the 2^1A state. There is some charge transfer already in the nontwisted conformation both in ABN and DMABN, but it is considerably enhanced by the twisting, such that the charge on the amino group increases from about +0.2e in the planar conformation to +0.6e at the twist angle 90°. The negative charge on the CN group increases by 0.1e on going from the ground to the 2^1A state in the nontwisted forms while the change is around 0.05e at the twisted geometries. The charge distribution is similar in the wagged and the nonwagged forms in both molecules, except that in the nonwagged form of the twisted DMABN the charge transfer is slightly smaller in the 2^1A state.

A final set of calculations were performed in order to shed some light on the alternative mechanism proposed by Zachariasse *et al.*[14,15,21,30] They proposed that a pyramidalization of the amino nitrogen could decouple the nitrogen lone pair from

(72) Gordon, R. D. *J. Chem. Phys.* **1990**, *93*, 6908.
(73) Berstein, E. R.; Grassian, V. H.; Warren, J. A. *J. Chem. Phys.* **1990**, *93*, 6910.

Table 5. Computed Energies,[a] Oscillator Strengths[b] (f), Dipole Moments[c] (μ), and effective Charges[c] on Each Subunit (NH_2 or NMe_2, Bz, and CN) of the Singlet States of ABN and DMABN at Several Geometries along the Wagging Coordinate (α)[d]

	ABN, 0° twist angle: $\alpha = 0°$						DMABN, 0° twist angle: $\alpha = 0°$					
state	ΔE	f	μ	NH_2	Bz	CN	ΔE	f	μ	NMe_2	Bz	CN
1^1A			6.89	−0.018	0.196	−0.178			7.36	−0.022	0.207	−0.185
1^1B	4.01	0.004	6.70	0.029	0.151	−0.180	4.05	0.010	7.58	0.050	0.129	−0.179
2^1A	4.44	0.361	12.42	0.228	0.006	−0.234	4.41	0.416	13.79	0.309	−0.065	−0.244
	$\alpha = 10°$						$\alpha = 10°$					
1^1A			6.80	−0.015	0.192	−0.177			7.24	−0.022	0.200	−0.178
1^1B	4.08	0.003	6.59	0.029	0.151	−0.180	4.19	0.005	7.44	0.055	0.126	−0.181
2^1A	4.51	0.365	12.32	0.230	0.004	−0.234	4.38	0.510	13.58	0.301	−0.068	−0.233
	$\alpha = 21°$						$\alpha = 21°$					
1^1A			6.30	−0.023	0.198	−0.175			6.40	−0.036	0.197	−0.161
1^1B	4.17	0.002	6.06	0.004	0.176	−0.180	4.02	0.003	6.33	−0.007	0.164	−0.157
2^1A	4.54	0.358	12.08	0.199	0.048	−0.247	4.23	0.411	13.27	0.256	0.002	−0.258
	$\alpha = 34°$						$\alpha = 30°$					
1^1A			5.88	−0.055	0.227	−0.172			6.41	−0.088	0.259	−0.171
1^1B	4.34	0.002	5.62	−0.031	0.210	−0.179	4.07	0.001	6.34	−0.050	0.231	−0.181
2^1A	4.67	0.309	11.51	0.179	0.049	−0.228	4.65	0.396	12.78	0.233	−0.007	−0.226
	$\alpha = 45°$						$\alpha = 40°$					
1^1A			5.50	−0.093	0.262	−0.169			6.10	−0.107	0.274	−0.167
1^1B	4.21	0.000	5.18	−0.079	0.258	−0.179	4.42	0.000	5.93	−0.088	0.268	−0.180
2^1A	4.74	0.340	11.00	0.131	0.093	−0.224	4.48	0.334	12.05	0.175	−0.046	−0.221

[a] Energies (ΔE) at the CASPT2 level (eV). [b] Oscillator strengths computed with CASSCF transition moments and CASPT2 energies. [c] Dipole moments and effective charges at the CASSCF level (D). [d] See Figure 5.

the π electrons of the phenyl ring and lead to an increase in the localization of the positive charge on the amino group in such a way that the dipole moment of the CT state could reach the high measured values (around 16 D in DMABN). In such a model, the inversion of the amino group should be the promoting mode for the ICT reaction instead of the rotation of the amino group. We have computed the energies, oscillator strengths, dipole moments, and effective charges of the lowest singlet states of both ABN and DMABN molecules at the non-twisted conformation along the wagging coordinate. The results are presented in Table 5 and Figure 4.

The ground state in ABN has, as was discussed in section 3.1, a minimum around a wagging angle of 17°. The inversion barrier is estimated to be around 2 kcal/mol. The 1^1B and 2^1A states (strictly S_1 and S_2) in ABN have minima at the nonwagged structure and both of them destabilize with respect to this conformation along the wagging angle, mainly above 20°, while only a slight increase of energy occurs up to this angle (less than 0.08 eV). The nonwagged form also has the highest dipole moment and the lowest effective charge on the amino group in both states. In particular, the 2^1A state has a dipole moment of 12.42 D and an effective charge on the NH_2 group of +0.23e. These values slightly decrease with the wagging angle. Similar trends can be found in DMABN. The ground state has a minimum at 10°, with an approximate barrier to inversion of 3 kcal/mol. As an additional point we can estimate the rotational barrier computed for DMABN in its ground state and compare it with the experimentally estimated value of 7.3 kcal/mol.[74] A full geometry optimization is not made so it is only possible to arrive at an approximate estimate of the theoretical barrier. The computed rotation barrier in the ground state of DMABN is 6.8 kcal/mol, calculated as the difference between the ground state minimum (0° twisted and 10° wagged) and the lowest computed energy for the twisted ground state (90° twisted and 21° wagged). The destabilization with the wagging of the singlet states is more important in DMABN above 30° undoubtedly due to the steric hindrance of the substituent. The wagging angles used in the calculations were for DMABN 0, 10, 21, 30, and 40°. Both the 1^1B and 2^1A states have energy minima at a wagging angle of 10°, close to the conformation where the ground state minimum is expected both by experiment and theory (cf. section 3.1). The inversion barriers in these states are approximately 0.4 and 3.8 kcal/mol for 1^1B and 2^1A, respectively. At the nonwagged conformation, the 2^1A state has a dipole moment of 13.79 D and an effective charge on the $N(CH_3)_2$ group of +0.31e. These values change to 13.58 D and +0.30e at a wagging angle of 10° (energy minimum), where the oscillator strength of the excitation is also maximum: 0.51. Further increase of the angle only decreases the values of the three properties. The combination of these results with the previous twisting studies with two different wagging angles shows the general insensitivity of the 1^1B (LE) state to moderate wagging angles (less than 30°), while the CT state shows different behavior in ABN and DMABN. The wagging slightly stabilizes the 2^1A (CT) state in DMABN in the nontwisted geometries, but, while the state also stabilizes with the wagging motion in DMABN in the 90° twisted geometry, the opposite is observed in ABN, probably due to the different interaction between the lone-pair and the substituent groups. A major point is that the wagging of the amino group becomes more important for the energy of the 2^1A state (S_2 state at nontwisted geometries and S_1 state after some critical twist angle) with larger twist angles. The dipole moments and the effective charge on the amino group are, however, not sensitive to the wagging angle along any of the studied paths. A model in which the solvent interaction in the nontwisted polar 2^1A state is able to bring this state below the 1^1B and lead to the CT fluorescence is not supported by our calculations. The wagging motion, without twisting, seems unable to provide the highly polar state responsible for the CT fluorescence (dipole moment of 16 D). The charge transfer obtained at nontwisted geometries are not higher than +0.13e, and no further stabilization of the 2^1A state with the wagging occurs, which leads to a larger transfer of charge.

These results for the molecular and electronic structure for ABN and DMABN are in full accordance with the twisted intramolecular charge transfer model. The relationship between

(74) Mackenzie, R. K.; MacNicol, D. D. *Chem. Commun.* **1970**, 1299.

Table 6. Experimental and Previous Theoretical Excitation Energies (ΔE, eV), Oscillator Strengths (f), and Dipole Moments (μ, D) of ABN and DMABN[c]

p-Aminobenzonitrile (ABN)

		absorption ($\theta = 0°$)[a]				($\theta = 90°$)[a]
state		exp[b]	CNDO1	CNDO2	PPP	CNDO2
2^1A	ΔE	4.74	4.97	5.0	4.66	5.1
	f		0.285	0.29	0.77	0.0
	μ				8.0	
1^1B	ΔE	>4.0	4.28	4.3	4.38	4.4
	f		0.014	0.011	0.02	0.001
	μ				14.4	

(*p*-Dimethylamino)benzonitrile (DMABN)

		absorption ($\theta = 0°$)[a]								
state		exp[b]	CNDO1	CNDO2	CNDO3	CNDO4	INDO1	INDO2	PPP	CI
2^1A	ΔE	4.42	4.87	4.8	4.51	4.46	4.63	4.64	4.35	5.71
	f		0.242	0.30		0.269	0.335	0.609	0.79	
	μ	14				8.66	8.35		16.5	
1^1B	ΔE	>4.0	4.28	4.2	4.15	4.69	4.40	4.22	4.13	
	f		0.019	0.015		0.00	0.06	0.024	0.04	
	μ	10[d]				5.61	8.99		10.5	

		emis. ($\theta = 90°$)[a]						
state		exp[b]	CNDO1	CNDO2	CNDO3	CNDO4	INDO1	CI
2^1A	ΔE	3.22	4.71	4.5	4.26	4.98	4.20	6.58
	f		0.00	0.00		0.00	0.00	
	μ	15				14.57	14.0	
1^1B	ΔE	3.6	4.48	4.4	4.51	4.42	4.85	6.05
	f		0.013	0.003		0.00	0.0001	
	μ					3.23	5.41	

[a] Theoretical results at the corresponding twisting angle. Experimental data tentatively assigned. [b] Experimental data from refs 6, 14, 26, 30, 35, 39, 75. [c] References: CNDO1,[6] CNDO2,[37] CNDO3,[40] CNDO4,[41] INDO1,[39] INDO2,[77] PPP,[76] CI.[43] [d] See text for a discussion of this value.

the present theoretical results and the TICT model will be discussed in detail in the next section.

3.4. The Triplet States Potential Curves for ABN and DMABN. Table 3 also gives the excitation energies and dipole moments computed for the two lowest triplet excited states. No evidence of a charge transfer process has been found for them. They are characterized as benzenoid-like states at all geometries studied here. This is in agreement with experimental evidence,[18,26] which indicates that the triplet states have low polarity and have geometries similar to the ground states. It has also been found that phosphorescence emission often occurs at energies above the TICT fluorescence,[26] which is in agreement with the theoretical results. As can be seen in Table 3, the 1^3A state potential curve has a minimum in DMABN at the ground state geometry, where the excitation energy is 3.50 eV. At the 90° twisted conformation this energy has increased to 3.92 eV and is now above the TICT state. Thus, the lowest state in DMABN at 90° twist angle is the singlet state, with the caution that the accuracy of the calculation provides.

The dipole moments for both triplet states decrease with the TICT angle. Schuddeboom *et al.*[30] have measured the dipole moment for the lowest triplet state. The value was found to be about 12 D independently of the solvent. It was concluded that DMABN does not undergo intramolecular charge transfer in the triplet state. Even though this conclusion is in accordance with the present theoretical results we note that the measured dipole moment is considerably larger than that obtained here (cf. Table 3), except for 1^3B at the wagging angle zero. The theoretical values are not expected to be in error with more than about 10% (as indicated by the results obtained for the singlet states). Therefore, in order to obtain agreement between theory and experiment for the dipole moment of the triplet state one has to conclude that the measurements were made for the 1^3B state. Although at the structures used in the calculation the 1^3B state is the second in energy, the differences in energy are within the accuracy of the method. Adiabatically it is also possible that the 1^3B state is actually the lowest triplet state. The dipole moment is strongly dependent on the wagging angle, so a further conclusion would be that the molecule is planar in this electronic state. The large value of the dipole moment must also imply some charge transfer in the 1^3B state, as is also born out by the population analysis (cf. Table 4). Note, however, that this polarity decreases with increasing twist angle. An alternative explanation for the experimental determination would be that the charge distribution in the excited state is very sensitive to the solvent polarization, but if this was the case one should expect the value of the dipole moment to be strongly dependent on solvent polarity, which does not seem to be the case.

As a final calculation we have computed the triplet state corresponding to the singlet TICT state. Bonacić-Koutecký and Michl[46] also found this state in the BH_2NH_2 molecule slightly above the singlet TICT state at the perpendicular geometry. In our present calculations on 21° wagged DMABN the triplet A TICT state appears at 4.03 eV, 0.3 eV above the singlet TICT state and 0.1 eV above the 1^3A state. This 2^3A TICT state has a dipole moment of 15.45 D and an effective charge on the amino group of +0.65e.

4. Discussion

Experimental data for the absorption and emission spectra of ABN and DMABN are presented in Table 6 together with information from previous theoretical studies. The absorption spectra of the two molecules are similar. The absorption spectrum of ABN in *n*-heptane has two distinct bands, one relatively weak starting around 4.0 eV (S_1) and a strong and structureless band peaking at 4.74 eV (S_2).[14] For DMABN the two bands nearly overlap, and the two absorption maxima occur

above 4.00 (S_1)[14,75] and at 4.42 eV (S_2).[14] In a more polar solvent as diethyl ether the more intense band is red-shifted by 0.1 eV. This has been used as evidence for a certain charge-transfer character and a large dipole moment of the S_2 state. The energy gap between the two states is smaller in DMABN than in ABN, which has been suggested[14,15] as one of the reasons for the dual fluorescence, since this distance will affect the size of the vibronic coupling between S_1 and S_2.

The fluorescence spectra give two bands for DMABN. In a nonpolar solvent such as cyclohexane, the "normal" fluorescence band (LE) is reported at 3.6 eV[30] (3.8 eV in alkanes[21]), and the second lower-energy band (CT) is found at 3.22 eV[30] as a very weak shoulder. The intensity of the CT band is strongly increased, and the energy decreased on going from nonpolar solvents to polar solvents like *p*-dioxane, as has been illustrated reiteratively for a number of solvents.[18] While the CT band gains in relative intensity in highly polar media, the energy of the LE band remains comparatively insensitive to an increase of the solvent polarity. Further, evidence exists that CT/LE fluorescence intensity ratio enhances when the substituents on the nitrogen are larger alkyl chains.[30] In ABN only the LE fluorescence takes place, which has been proven by analysis of the decay curves in several different solvents.[14] Both bands are in DMABN independent of concentration and excitation wavelength over a large range, although the concentration in DMABN has to be kept low to prevent dimer formation[21] and certain dependence of the excited states properties on concentration occur below 296 nm.[7,21] The fluorescence quantum yields for the LE transitions in both molecules depend on the solvent polarity, although the variation is larger in DMABN, probably due to the presence of the CT band. The quantum yield in the ABN LE band undergoes a small decrease and the DMABN LE band quantum yield strongly decreases with an increasing polarity of the environment, while the CT band quantum yield consequently increases.[30] The temperature has an important effect on the two bands. An increase of the total quantum yield fluorescence with temperature has been reported.[18] A slight increase of the quantum yield of the CT fluorescence with temperature[18] is attributed to the Franck–Condon forbidden nature of the transition due to the lack of orbital and vibrational overlap.[78,79] Likewise, recent experiments[30] have shown that the CT/LE quantum yield ratio and rate constants decrease with temperature.

The first full analysis of the forward and backward ICT reactions in DMABN were performed by Zachariasse *et al.*[13] when the time resolution and dynamic power of the laser equipments allowed meaningful analysis of the decay curves and direct measurements of rate constants. Determination of the activation energies of the ICT formation could be carried out.[13] The results were in contrast with previous studies, which were more consistent with a barrierless model.[18] It has also been shown that the reverse reaction has a barrier with an activation energy higher than that of the solvent mobility.[18,80] The activation energy for the ICT formation in DMABN has been measured to be around 1.9 kcal/mol in toluene,[30] and 1.2, 2.3, 3.2, and 4.7 kcal/mol in the solvent series from diethyl ether to dipentyl ether,[21] an important decrease of the activation energy with the polarity of the solvent. The experimental data on the activation energy refers to the reaction from the LE to the CT state. We show that the 2^1A state has no potential energy barrier along the twisting coordinate on going from 0 to 90°. This does not mean, however, that our theoretical results support a barrierless mechanism. In a simple model we would compute the activation energy as the energy difference between the minimum of the optimized 1^1B state (responsible of the LE fluorescence) and the energy maximum in the path going from the LE minimum to the CT minimum. As a rough approximation we can estimate such a barrier from the S_1 potential energy curve of Figure 3 (wg0 and wg21) which is computed to be 4.8 kcal/mol. The actual value for the gas-phase system ought therefore to be higher when the LE state is fully optimized. The decrease of the barrier height when increasing the polarity of the solvent confirms the two state model, independently of a given twisting or wagging mechanism, due to the strong stabilization of the polar 2^1A state.

Table 7. Summary of Experimental and Computed Excitation Energies (eV), Oscillator Strengths (*f*), and Dipole Moments (μ, D) of ABN and DMABN[a]

	absorption					emission (F_A band)[c]				
	energies		*f*	dipole		energies		*f*	dipole	
state	exp[d]	theo	theo	exp[e]	theo	exp[f]	theo	theo	exp[e]	theo
					p-Aminobenzonitrile (ABN)					
1^1A				6.6	6.30					
1^1B	>4.0	4.17	0.002		6.06					
2^1A	4.74	4.54	0.357		12.00		3.82	0.0		15.75
					p-Dimethylaminobenzonitrile (DMABN)					
1^1A				6.6	7.24					
1^1B	>4.0	4.19	0.005	10[g]	7.44					
2^1A	4.42	4.38	0.510	14	13.58	3.22	3.74	0.0	15	15.45

[a] Theoretical energies at the CASPT2 level, μ at the CASSCF level, and *f* computed using the CASSI approach and CASPT2 excitation energies. [b] The theoretical geometries used are the ground state minimal energy structures: ABN, 0° twisted and 21° wagged and DMABN, 0° twisted and 10° wagged. [c] Minimal energy structures used for the CT state: ABN, 90° twisted and 0° wagged and DMABN, 90° twisted and 21° wagged. [d] Values in *n*-heptane, band maxima, ref 14. [e] References 26 and 30. [f] Values in the nonpolar solvent cyclohexane, ref 30. Around 3.8–3.9 eV has been measured in alkanes. The gas-phase value, if were possible, should be expected at higher energy. [g] See text for a discussion of this value.

Our computed results (cf. Figure 2 and 4 and Tables 3 and 5) agree with most of the experimental evidence and suggest the twisted intramolecular charge transfer mechanism as the most suited model to explain the dual fluorescence occurring in aminobenzonitriles. The wagging model is uncapable of producing a highly polar state, which can explain the charge transfer. It is important to note that the photophysical behavior of the systems we are dealing with is complex. For instance, it is expected that in DMABN in alcohol solutions new photophysical processes take place.[7,21,80] Other systems present different photophysical phenomena,[13–15] and it is difficult to include all the experimental evidence in a global model. The experimental and our computed energies and dipole moments in both molecules are summarized in Table 7. The absorption energies deviate by less than −0.2 eV from the experimental data in nonpolar solvents. The computed absorption energies at the ground state minima (nontwisted conformation) are vertical transitions, and therefore they can be compared to energies for band maxima, which are generally believed to be close to computed vertical excitation energies. The 2^1A state appears above the 1^1B state with an expected larger value for

(75) Herbish, J.; Pérez-Salgado, F.; Rettschnick, R. P. H.; Grabowski, Z. R.; Wójtovicz, H. *J. Chem. Phys.* **1991**, *95*, 3491.
(76) Gordon, M. D. *Tetrahedron* **1980**, *36*, 2113.
(77) Herbish, J.; Rotkiewicz, K.; Waluk, J.; Andresen, B.; Thulstrup, E. W. *Chem. Phys.* **1989**, *138*, 105.
(78) Grabowski, Z. R.; Rotkiewicz, K.; Rubaszewska, W.; Kirkor-Kamińska, E. *Acta Phys. Polon.* **1978**, *A54*, 767.
(79) Van der Auweraer, M.; Grabowski, Z. R.; Rettig, W. *J. Phys. Chem.* **1991**, *95*, 2083.
(80) Heisel, F.; Miehé, J. A.; Martinho, J. M. G. *Chem. Phys.* **1985**, *98*, 243.

the oscillator strength. At the twisted conformation the results matches with the lower-energy fluorescence. The observed value for the A band in DMABN ranges from 2.7 to 3.22 eV on going from more to less polar solvents,[14,18] It is expected that a corresponding gas-phase value will be close to the computed energy, 3.74 eV. This value is below the 3.84 eV obtained for LE fluorescence in toluene,[13] and higher values are expected for less polar solvents. This fact could be in contradiction with the well-known absence of dual fluorescence in the gas-phase DMABN[14,18] and even with the slightly positive or zero value for ΔH found for DMABN in alkanes.[21] The results is, however, within the error limits expected for our calculations (0.2−0.3 eV) in such a system, and the energy value for the 2^1A state at the 90° twisting angle could be slightly higher. The absence of fluorescence in the gas-phase DMABN is probably related to a behavior controlled by the vibrational redistribution *versus* relaxation dynamics. In the condensed phase the system is moving more or less on the potential hypersurface (plus tunneling). In the free molecule, even at sufficient excess of excitation energy over the 0−0 transition, the dynamics of the energy distribution, in absence of a heat bath or collisions to allow an energy loss, can disfavor the vibrational mode critical for the process.[22] Only a decrease of the activation barrier by the solvent interaction with the polar state seems to allow the reaction. The ICT mechanism in DMABN has been measured as a exothermic process with standard enthalpies depending on the solvent: −5.4 kcal/mol in *n*-butylcloride,[26] −3.5, −2.7, −2.1, and −0.9 kcal/mol in the series from diethyl ether to dipentyl ether,[21] and −1.4 kcal/mol in toluene,[13] showing an important increase of the enthalpy due to the stabilization of the ICT state for more polar solvents.

Electro-optical absorption and emission measurements[28] on DMABN and related compounds proved that the magnitude of the dipole moment of the CT state (μ_a) is about three times larger than the dipole moment (μ_b) of the almost planar fluorescing LE state, but the dipole moment of the absorbing Franck−Condon S_2 ($\mu^{FC}{}_a$) state is of similar magnitude as that of μ_a.[18] These results are in agreement with the calculations as illustrated in Figures 2 and 3 and shown in Table 3 both for the wagged and non-wagged geometries. The computed dipole moment of the 1^1B state in wagged DMABN varies from 6.33 D at the non-twisted geometry to 4.87 D in the perpendicular form. On the other hand, the absorbing Franck−Condon 2^1A state has a computed dipole moment at the ground state geometry of 13.27 D, in agreement with the experimental estimate: 11−14 D.[26] The state has a computed dipole moment of 15.45 D at the 90° twisted conformation, also in agreement with the experimental measurements, which yield 15−16 D,[26,30] which is somewhat larger than the value obtained at the non-twisted geometry, as the calculations suggest. The LE band is less sensitive to solvent polarity. The maximum of the band in DMABN decreases with solvent polarity from 3.62 eV in *n*-hexane ($\epsilon = 1.88$) to 3.48 eV in 1,2-dicloroethane ($\epsilon = 10.4$).[21] This small sensitivity and the measured wavelength-dependent decay curves suggest that the dipole moments in the ground and in the excited 1^1B states are in the same direction and not very different.[18] In DMABN, however, the measured dipole moment of the state responsible for the LE transition is around 10 D, while the overall dipole moment goes from 9.9 D in cyclohexane to 15.1 D in *p*-dioxane due to the increasing participation of the ICT state with the polarity of the solvent.[30] It is important to mention that we have not computed the LE state minimum, and, therefore, the dipole moments computed for the 1^1B state are not strictly comparable with the experimental data.

A possible argument against the TICT mechanism is the decrease of the rate constant for intramolecular charge transfer when the size of the substituent on the nitrogen increases,[14,15] which is an unexpected effect if the rotational isomerism around the *N*-phenyl bond would be the rate-determining step, although it perfectly correlates with the increase of the nitrogen inversion barrier with decreasing substituent size. Nevertheless, the observed trends in the rate constant values do not invalidate the TICT model, especially since it has been shown that many strongly hindered systems are twisted already in the ground state. For instance, *p*-pyrrolidinebenzonitrile reacts slower toward the TICT state than 2,5-dimethyl-*p*-pyrrolidinebenzonitrile by a factor of 1.8, although the rotational volume of the latter is larger due to the two additional methyl groups. This fact would argue against the kinetic expectations, but it has been shown that the larger compound is around 10° more twisted in the ground state than the unsubstituted compounds.[25,81] An increased twisting angle in the ground state can also increase the fluorescence rate constant, because the initial twisting angle favors the twisting mechanism. Other factors, such as the interaction with the surrounding dielectric, the shape of the potential energy surfaces, and the energy gap between the S_1 and S_2 states can be even more important in determining the kinetics of the twisting mechanism.[81] When the energy gap between the 1^1B and 2^1A states is reduced, the activation barrier for the ICT reaction strongly decreases, as has been shown by Zachariasse *et al.*[14,15] The values for the activation energies are larger in less polar solvents as expected by the theoretical model (cf. Figure 3) and is due to the sensitivity of the 2^1A state to the solvent polarity. This is the observed trend in recent studies, as has been discussed above for toluene and the dialkyl ether series. It should be noted that, due to the important role of the solvent polarity, a definitive relationship between activation energies and viscosity has not been established.[18,21,32−34]

Table 6 also gives some data from previous theoretical studies performed on the ABN and DMABN systems. The general features are the same in most of them, for instance, that the 2^1A state is higher than the 1^1B state at the planar form and lower at the twisted geometry. Exceptions are the earlier semiempirical CNDO calculations and the CI study. The oscillator strengths follow the expected trends, with large values for the 2^1A state at the planar form and zero at the twisted conformation. The computed dipole moments are in agreement with the CASSCF values, except for the high dipole moments of the 1^1B state in the planar form in the PPP and INDO calculations. It may, however, be noted that the CASSCF dipole moment for the 1^1B state is somewhat larger for zero wagging angle than when the angle is 21° (7.58 *versus* 6.33 D).

Therefore, the present theoretical study supports the suggested formation of a twisted ICT state in the DMABN molecule, in agreement with a large amount of experimental data.[18] Recent experimental evidence, able to handle the short picosecond decay times,[13] have questioned some of the previous experimental data and put forward evidence against the twisting model. No alternative mechanism, as for example the wagging of the dimethylamino group in DMABN, seems to match better with the present results, which, of course, does not completely rule out that such a type of mechanisms may be competitive, in particular if the twisting cannot take place due to molecular bridging[14] or high activation barriers. The ABN molecule, where no evidence of dual fluorescence has been presented in any solvent, has an energy barrier which prevents the twist of the amino group. The structure and shape of the 2^1A potential

(81) LaFemina, J. P.; Duke, C. B.; Rettig, W. *Chem. Phys.* **1990**, *147*, 343.

curve along the twist coordinate has been shown to be related to the character of the HOMO → LUMO and n → π^* electron configuration. From the ionization potentials of methylanilines discussed in the previous section, this n → π^* state is expected to lie around 1 eV higher in the nontwisted conformation in ABN than in DMABN. In the nonwagged molecule (Figure 2, wg0), a strong avoided crossing occurs around 60° of twisting in ABN due to the relative position of these two ^{1}A states. In the wagged molecule (Figure 2, wg21), the energy barrier to the rotation is not so important and, furthermore, there is no stabilization of the state at 90°. The high energy of the "pure" lone pair (lpN) → LUMO state at the non-twisted geometry implies that the 2^1A state does neither stabilize nor couple with the 1^1B state along the rotation until at large twisting angles, preventing in this way the appearance of CT fluorescence. The change of hybridization of the nitrogen atom can also be related to the intramolecular charge transfer process. At the planar conformation the hybridization is sp^2, and no further interactions are expected for the lone-pair orbital except with the benzonitrile π_x orbitals. In wagged DMABN molecules, however, pyramidalization of the nitrogen atom gives a lone-pair orbital with sp^3 hybridization. Unlike ABN, in DMABN the lone-pair orbital can interact with the orbitals of the methyl groups, although weakly in the nonwagged form. This interaction remains during the twisting process and could explain the increased mobility of the lone-pair electrons in DMABN compared to ABN. The increased interaction leads to the presence of dual fluorescence in DMABN in contrast to ABN. Likewise, the energy gap between the 1^1B and 2^1A states determines the shape of the potential curves, leading to a stronger coupling in DMABN and a weaker coupling in ABN.

Three states are mainly involved in the characteristic shape of the low-lying singlet excited states in both molecules. First, the energy gap between the ^{1}A HOMO → LUMO and ^{1}A lpN → LUMO states modifies the S_2 behavior by an avoided crossing. The lpN → LUMO (CT) state tends to strongly stabilize along the twisting coordinate (cf. section 3.2), while the HOMO → LUMO state destabilizes. The general destabilization of the ^{1}A HOMO → LUMO state until the crossing with the higher state of the same symmetry can be understood, because the "pure" HOMO → LUMO state is a benzonitrile-like state, as the ground and 1^1B states, which also destabilize. A lower CT state at non-twisted geometries strongly interacts with the 2^1A state, and, therefore, the latter state can stabilize along the twisting, as happens in DMABN. If the shift is larger, as expected in ABN by the ionization potentials and the energies of the lone-pair orbital, the avoided crossing between the two ^{1}A states will occur at a larger twisting angle. The destabilization of the 2^1A state is higher at this point, and, therefore, the potential energy barrier is also higher (cf. Figure 2). On the other hand, the energy gap between the 1^1B and 2^1A (S_1 and S_2) states at non-twisted geometries will be the determining factor to model the shape of the S_1 surface along the isomerization coordinate, where the ICT reaction is expected. Small values in this energy gap lead to crossing in the hypersurface with small geometric changes and, moreover, small activation barriers on S_1 (cf. Figure 3, wg21). Larger gaps imply that the crossing takes place after further evolutions along the potential energy surface and larger barrier heights can be expected (Figure 2).

This explanation would support the observed trends in molecules with larger substituents on the nitrogen, both alkyl or cyclic groups, where the two states decrease the energy gap and therefore the activation energies along the reaction path and where the dual fluorescence appears more clearly. Also, the presence of substituents on the benzene ring as, for instance, in the *o*- and *m*-DMABN inhibits the dual fluorescence.[14] The absorption spectra of these two molecules show that the S_1 and the S_2 bands are clearly separated[82] with a gap even larger than that found in ABN and MABN.[14] The combination of both the oxidation potentials of the molecules (cf. section 3.2) and the energy gaps measured in absorption for the S_1 and S_2 states can be used in a simple model as a qualitative way to predict the occurrence of dual fluorescence in similar systems. Anyway, the effects of the solvent on the activation energy of the ICT reaction will be a determining step for the occurrence of the phenomenon.

5. Summary and Conclusions

In this article, results have been presented of a theoretical study at the CASSCF and CASPT2 level of theory for the *p*-aminobenzonitrile (ABN) and (*p*-dimethylamino)benzonitrile (DMABN) molecules, which was performed in order to get more insight into the dual fluorescence phenomenon occurring in these systems. The latter molecule has been shown to present two fluorescence bands in polar solvents, while no evidence for a second lower-energy fluorescence band has been found in ABN. The most suited model proposed to explain the dual emission is a twisted intramolecular charge transfer mechanism where the alkylamino group twist in an initially promoted excited state from the non-twisted conformation of the ground state toward a new geometrical arrangement of the molecular subunits where the amino group is perpendicular to the benzonitrile moiety. This excited state is characterized by a large charge separation making the lower-energy fluorescence band strongly sensitive to the solvent polarity. The model is known as the TICT mechanism,[16-18] and it has been supported by a large number of experimental studies,[18] although it has been questioned by recent experiments[14,15]

The present calculations comprise the low-lying singlet and triplet excited states of the above molecules computed at the geometry of the ground state and at the geometries obtained by twisting the amino group with respect to the benzonitrile plane 30, 60, and 90°. Initially, the geometries of the ground states were optimized at the CASSCF level. The energies of the excited states were computed at the CASPT2 level for the four geometries in the two molecules, both using a wagging angle of 0 and 21° to account for the effect of the wagging angle along the twisting. Further, calculations on ABN and DMABN molecules along the wagging corodinate at the nontwisted geometry were performed on the ground and low-lying singlet excited states in order to analyze the suggested influence of the amino group wagging motion on the mechanism. The results perfectly match with the main features of the TICT process and not with the wagging process since inversion is unable to produce the charge transfer state that is responsible of the lower-energy fluorescence in aminobezonitriles. The absorption energies have been calculated to be within ±0.2 eV of the experimental results obtained in the non-polar solvents. The computed potential energy curves and properties are consistent with a promoted vertical S_2 state with a dipole moment around 13 D, higher in energy than the weakly allowed S_1 state. The S_2 state will carry most of the excitation energy due to its strongly allowed Franck–Condon character. The suggested double mechanism for fluorescence would occur first via the deactivation to the S_1 state. From the LE state (S_1 state at

(82) Seliskar, C. J.; Khalil, O. S.; McGlynn, S. P. In *Excited States*; Lim, E. C., Ed.; Academic Press: New York, 1974; Vol. 1, p 231.

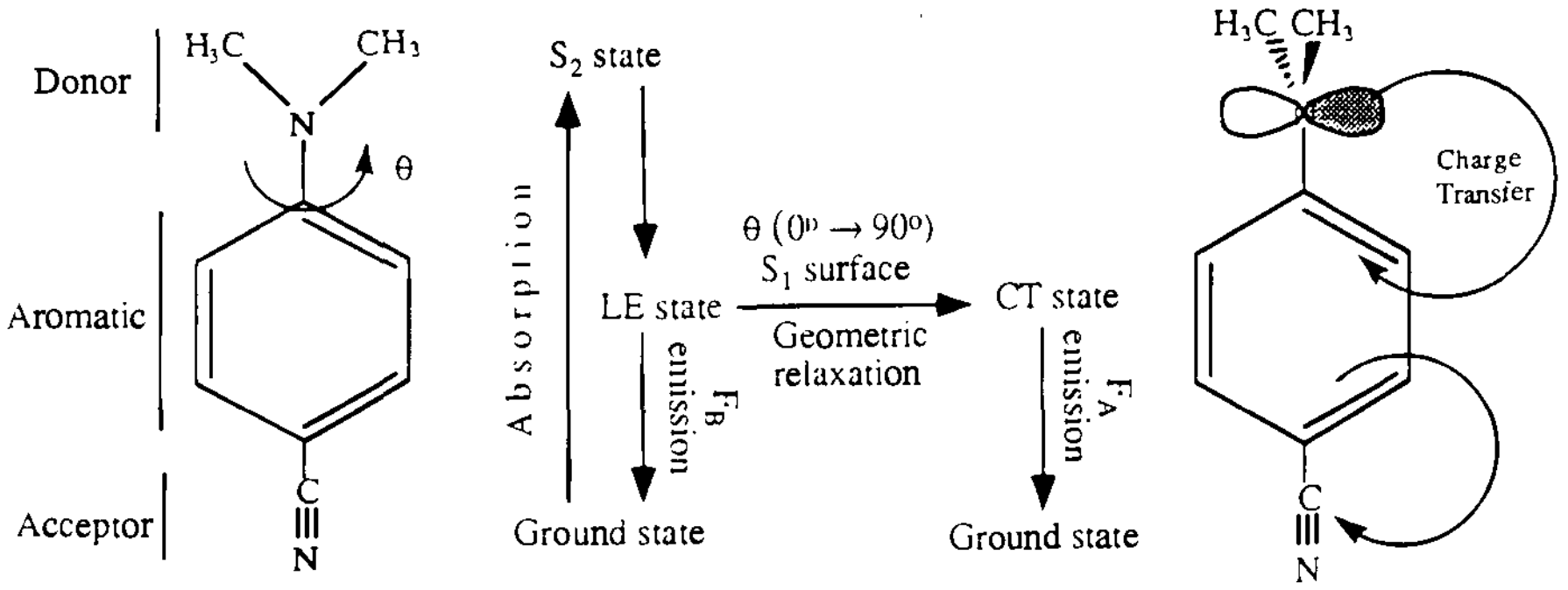

Figure 5. The dual fluorescence mechanism (TICT model) in DMABN.

geometries with small twist angles), an emission can take place (F_B fluorescence). Along the S_1 surface the adiabatic photoreaction, via intramolecular twisting motion, can also be achieved. The character of the S_1 state progressively changes from the initial LE state to the final CT state, from which the new emission occurs (F_A fluorescence). Figure 5 summarizes the proposed twisted intramolecular charge transfer process in DMABN from the absorption of the energy to the dual fluorescence. The corresponding process in ABN is hindered by the shape of the potential energy surface on the twist, mainly due to the energy gaps between the excited states at the excitation geometry. Computed properties for the different electronic states are in agreement with available experimental information.

To summarize, it seems that a requirement for the occurrence of dual fluorescence and ICT in aminobenzonitriles and related molecules is a small energy gap between the interacting states, as was suggested by Zachariasse *et al.*[14,15] The isomerization leading to a twisted conformation of the amino group describes very well the charge transfer state responsible for the long-wavelength fluorescence appearing in solution.

Acknowledgment. The research reported has been supported by a grant from the Swedish Natural Science Research Council, by IBM Sweden under a joint strudy contract, by the Cooperación Científica y Técnica of Ministerio de Asuntos Exteriores of Spain, and by projects PB91-0634 of the Dirección General de Investigación Científica y Técnica and OP90-0042 of the Secretaría de Estado de Universidades e Investigación. L.S.A wishes to thank the Ministerio de Educación y Ciencia for a personal grant. The authors are indebted to Prof. Klaas A. Zachariasse and Prof. Zbigniew R. Grabowski for helpful suggestions and discussions which have contributed to a better understanding of the experimental evidences and an improvement of the paper.

JA94I)440O